Journal of the European Ceramic Society 44 (2024) 23–42

Contents lists available at ScienceDirect

Journal of the European Ceramic Society

journal homepage: www.elsevier.com/locate/jeurceramsoc

Review on the strategies to improve the mechanical strength of highly porous bone bioceramic scaffolds

Zahra Miri [a], Håvard Jostein Haugen [b], Dagnija Loca [c,d], Filippo Rossi [e], Giuseppe Perale [f,g,h], Amirhossein Moghanian [i], Qianli Ma [b,j,*]

[a] Faculty of Medicine and Health Technology, Tampere University, 33100 Tampere, Finland
[b] Department of Biomaterials, Institute of Clinical Dentistry, University of Oslo, NO-0317 Oslo, Norway
[c] Rudolfs Cimdins Riga Biomaterials Innovations and Development Centre of RTU, Institute of General Chemical Engineering, Faculty of Materials Science and Applied Chemistry, Riga Technical University, LV-1007 Riga, Latvia
[d] Baltic Biomaterials Centre of Excellence, Headquarters at Riga Technical University, Riga, Latvia
[e] Department of Chemistry, Materials and Chemical Engineering "Giulio Natta", Politecnico di Milano, via Mancinelli 7, 20131 Milano, Italy
[f] Industrie Biomediche Insubri SA, Mezzovico-Vira 6805, Switzerland
[g] Faculty of Biomedical Sciences, Università della Svizzera Italiana (USI), Lugano 6900, Switzerland
[h] Ludwig Boltzmann Institute for Experimental and Clinical Traumatology, Vienna 1200, Austria
[i] Department of Materials Engineering, Imam Khomeini International University, Qazvin 34149–16818, Iran
[j] Department of Immunology, School of Basic Medicine, Fourth Military Medical University, Xi'an 710032, PR China

ARTICLE INFO

Keywords:
Mechanical properties
Bone scaffolds
Porous scaffold
Bioceramics
High-strength scaffolds

ABSTRACT

Bone healing is an impressive ability of the human body, but critical-sized bone defects require external intervention. Bioceramic scaffolds with excellent biocompatibility and bioactivity have been developed to treat non-healing bone defects because of their unique features for bone repair. Meanwhile, the mechanical properties of the material continue to be disadvantageous. This review focuses on (i) essential factors in affecting and improving bioceramic-based scaffolds' mechanical properties, including porosity, pore size, methods, and material composition, and (ii) summarizing previous studies and highlighting strategies to fabricate scaffolds with improved mechanical properties such as using nano-particles, using a combination of bioceramics and polymers, and modifying scaffold surfaces. Further research is necessary to improve bioceramic scaffolds for bone repair applications.

1. Introduction

Bone contains both organic and inorganic components. Approximately 8–10 % of bone consists of water, 60% is dedicated to the inorganic phase, and the remaining percentage is for organic components [1]. Bone's organic part mainly comprises collagen type I, diverse non-collagenous proteins, and cells (approximately 2 %) [1]. This part is essential for bone performance and can profoundly affect some bone properties, including biochemical and mechanical properties. Collagen of type I is composed of a sequence of three polypeptide chains. The structure results in the creation of a rigid layer of molecules whose length is nearly 300 nm. Each molecule is placed adjacent to the next to create a collagen fibril. Afterward, these fibrils form bundles to create a group of collagen fibers [2,3]. Bone has a mineralized framework consisting of calcium salts and collagen fibers. The mineral component includes calcium hydroxyapatite, calcium carbonate, and magnesium phosphate. Bone is divided into two types –cortical and trabecular-each-each with a distinct structure, as shown in Fig. 1.

Bone has a high capacity for regeneration. Most fractures can be quickly healed with simple internal/external fixation [4]. Despite this superior property, the bone's ability for self-healing can be limited depending on the damage's extent. Therefore, it can heal minor damage, but a critical-sized defect, such as a segment bone defect (SBD) [5], is challenging to heal. As a porous structure, scaffolds provide a mechanical and structural substrate to support cell growth [6] for tissue engineering (TE). The interconnected structure of scaffolds allows oxygen and nutrition to migrate from the scaffolds' surface to the inner part [7]. In addition, the porous architecture provides more surface area for the cells and scaffold's interaction [8]. An ideal bone engineering scaffold should meet the following requirements [9,10]:

* Corresponding author at: Department of Biomaterials, Institute of Clinical Dentistry, University of Oslo, NO-0317 Oslo, Norway.
E-mail address: qianlima@odont.uio.no (Q. Ma).

https://doi.org/10.1016/j.jeurceramsoc.2023.09.003
Received 22 May 2023; Received in revised form 9 August 2023; Accepted 2 September 2023
Available online 9 September 2023

- Biocompatibility: The scaffold material should be non-toxic and not cause adverse host responses in the body.
- Bioactivity: The scaffold should have the ability to encourage bone regeneration by stimulating the growth and differentiation of bone cells.
- Porosity: The scaffold should have a high porosity to allow the vascularization and exchange of nutrients, oxygen, and waste products, which is essential for cell growth and metabolism.
- Mechanical properties: The scaffold should have appropriate mechanical properties that can support the weight of the surrounding tissues and withstand mechanical loading during bone regeneration.
- Biodegradability: The scaffold should be biodegradable and undergo gradual degradation over time, allowing for natural tissue replacement.
- Structural stability: The scaffold should maintain its structural integrity during the initial stages of bone formation, guiding bone formation.

The ideal scaffold for bone engineering should also be versatile and customizable, allowing it to be tailored to individual patients' needs and readily accessible in the clinic or operating room [11]. Mechanical properties, architecture, and osteogenic ability are other essential characteristics of a desirable scaffold [12]. A recent review indicated that mechanical loadings significantly impact initial bone healing and bone remodeling after bone fracture/trauma [13]. Being exposed to various mechanical loadings after implantation, such as tension, shearing, compression, and torsion, The *in-vivo* performance of scaffolds is greatly affected by their mechanical properties, by which scaffolds can withstand skeletal weight and motion [14].

A non-smooth surface is beneficial for properly integrating the scaffold as it can enhance the proliferation, attachment, and differentiation of adherent bone-forming cells. Also, they should endure the mechanical stimuli generated by the environment, especially in load-bearing conditions [15–17]. The mechanical strength of the scaffold is evaluated based on its ability to withstand impact and maintain its integrity during implantation [18]. When analyzing the mechanical properties of bone, it is important to consider factors such as toughness, shear modulus, Young`s modulus, fatigue strength, compressive strength, and tensile strength. Although various tests have been established to evaluate these properties, the most frequently used methods for scaffold assessment are tensile and compressive tests. To ensure that scaffolds have mechanical properties similar to those of the native tissue or organ and to avoid adverse effects resulting from the stress-shielding mechanism, it is necessary to determine an appropriate range of mechanical properties for each application during tissue remodeling. Mimicking these mechanical properties for the scaffolds at both the fabrication and implantation stages is essential to making scaffolds a good candidate for bone regeneration [19].

Materials for fabricating scaffolds should be non-cytotoxic and facilitate cells' functions such as differentiation and proliferation [8]. In this regard, several materials (synthetic or/natural, permanent or bioresorbable) have been engineered and investigated to fabricate scaffolds. 'Bioactive' scaffolds can actively encourage bone in-growth by interacting with the surrounding tissue. Due to their composition resembling that of the inorganic portion of bone, "bioactive" ceramics (calcium sulfate, calcium phosphates, etc.) and bioglasses (45S5, 6P53B, 13–93, etc.) have great osteoconductivity [20], biodegradability, and osteoinductivity [21]. Bioceramics are an appropriate candidate since they show better performance (tissue response) compared to metals and polymers [22]. The deformation of ceramics through plastic means is challenging due to the nature of their bonds and the restricted amount of slip, as opposed to metals and polymers. As a result of these features, ceramics exhibit non-conductivity and almost zero creep when maintained at room temperature. So, ceramics tend to develop micro cracks and grooves due to their inability to tolerate plastic deformation from the cracking area. Rather than accommodating plastic deformation, they exhibit elasticity and are therefore susceptible to this type of damage. When a crack appears in ceramic materials, the stress at the tip of the crack is significantly greater than the stress in the surrounding material. This stress concentration weakens the ceramic, making it difficult to determine its compressive strength [23]. Bioactive glasses (BGs) and crystalline ceramics such as hydroxyapatite (HAp) and tricalcium phosphate (TCP) are also materials that promote bone growth by supporting the formation of new bone tissue [24–27]. BGs are implanted in defect sites, where ion exchange with the surrounding biological fluid causes a bone-like apatite layer deposition on implant surfaces. This process occurs due to interactions between the glass surface and the biological fluid, forming a favorable environment for apatite deposition. Given that apatite encourages the adhesion and proliferation of osteogenic cells, the bone partially replaces this biological apatite after long-term implantation [28–30]. However, despite their excellent bioactive characteristics, BGs and ceramics have poor mechanical strength and fracture toughness. Due to these properties, their use is often limited to non-load-bearing applications, but intelligent approaches partially resolve these issues. Various solutions are available to solve this drawback. Some polymers and materials, such as nanoparticles, nanodiamonds, etc., have been introduced for this aim. Therefore, because of the importance of mechanical properties, this study reviewed approaches associated with improving bioceramics scaffolds' mechanical properties. This review first briefly introduced bioceramics and, secondly, focused on the factors involved in improving the mechanical properties of scaffolds.

2. Bioceramics and bioglasses

Bioceramics are bioactive and biocompatible [32] materials that are useful for bone repair. Synthetic bioceramics possess outstanding features compared to polymers and metals, including bioactivity,

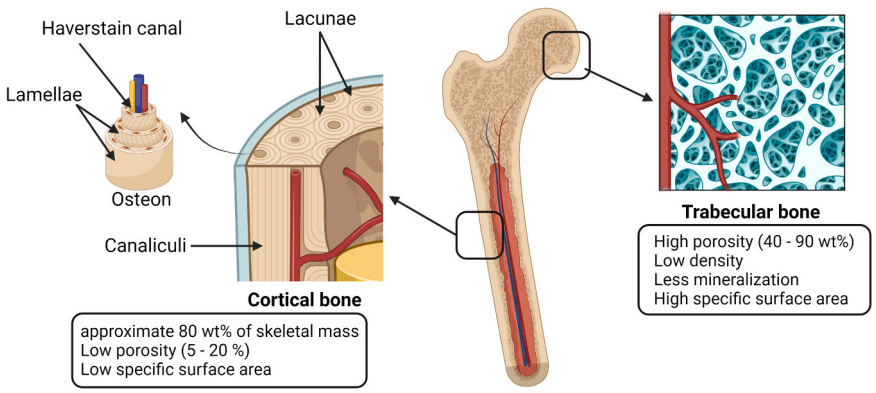

Fig. 1. The structure and properties of bones. Created by BioRender according to previous publication [31], with Publication License CG25OKGI5V.

biocompatibility, and strength. Hence, they are considered to have superior bone regeneration and repair [33,34]. Synthetic bioceramics decrease the danger of immune rejection and autograft morbidity. Moreover, there is a similarity between the porous bone structure and certain bioceramics, namely HAp and β tricalcium phosphate (β-TCP), used in this application [33]. This similarity causes osteoprogenitor cells' differentiation and bone matrix deposition; thus, bioceramics are considered osteoconductive [35]. Bioceramics are mainly categorized into bioinert, bioresorbable, and bioactive ceramics [36]. Generally, bioceramics comprise a diverse collection of calcium phosphate, which can be categorized based on their Ca/P molar ratio and compositions. Bioceramic materials include BGs (e.g., borate-, silicate-, phosphate-, borosilicate, mesoporous and doped BGs), calcium silicate (CS, e.g., β-calcium silicates, and tricalcium silicates), zirconia, alumina, β-tricalcium-phosphate (Ca/P: 1.5), α-tricalcium-phosphate (Ca/P: 1.5), HAp (Ca/P: 1.67), and calcium phosphates (CaPs) [37,38]. Bioceramics have several positive attributes, including their similarity to the inorganic part of bone tissue, excellent osteoconductivity, and ideal biocompatibility [39,40]. Nevertheless, their fragility may limit their use in critical bone defects [41]. Different categories have been described below:

2.1. Aluminum oxide (Al_2O_3)

Aluminum oxide (Al_2O_3), or alumina, is a highly utilized oxide ceramic in various engineering and biomedical fields. The majority of Al_2O_3 powder, a raw material, is generated by the Bayer process from bauxite. Its applications are vast and diverse. Al_2O_3 with a high level of purity labeled as 99.99% integrity is an increasingly favorable option in biomedical engineering, particularly for dental and orthopedic utilization, such as femoral components in total hip replacements. Al_2O_3 is recognized for its exceptional material properties, such as high hardness, low friction, excellent wear resistance, and good corrosion protection. These features make it an optimal choice for articulating surfaces in orthopedic applications [42]. Al_2O_3-based bioceramics were initially available as alternative components for hip joint prostheses and dental implants [43]. Al_2O_3 prostheses can also be employed in various clinical applications such as bone screws, ossicular (middle ear) bone substitutes, alveolar ridge (jaw bone) and maxillofacial reconstruction materials, segmental bone replacements, and substitutes for corneal etc. [21] Nevertheless, Al_2O_3 is easily prone to fracturing due to its poor toughness, which has been recognized as a drawback [44].

2.2. Zirconia

Zirconia is commonly employed for clinical purposes and implantation as partially stabilized zirconia (PSZ). PSZ offers multiple advantages over Al_2O_3, including higher flexural strength, fracture toughness, Weibull modulus for better reliability, lower Young's modulus, and ease of achieving a superior surface finish through polishing [42]. Zirconia has been reported to be biocompatible with the oral cavity tissues and osteoconductive, facilitating bone formation after implantation [45]. Zirconia ceramics have some drawbacks, such as their opacity, which can compromise esthetic properties and aging. Moisture accelerates this process, leading to degradation and increased surface roughness. Additionally, the cracks' presence may compromise long-term performance [37].

2.3. Calcium phosphates (CaPs)

Calcium phosphate (CaP) are bone-like materials naturally present in the body and have mineral components similar to calcified tissues. As a result, they have been proposed for various dental and orthopedic applications [46–48]. These bioceramics have noteworthy osteoconductivity, bioresorbability, and biocompatibility properties [49], allowing them to seamlessly integrate into living tissues through the same processes involved in bone remodeling. This process occurs when a portion of CaPs is dissolved in the surrounding microenvironment. As the liberated ions are released, proteins are attracted to the surface, and the precipitation of biological apatite crystals occurs, forming a layer on the biomaterial. Moreover, CaPs are easily obtained at a low cost and can be certified as medical grade relatively easily. The dissolving behavior of CaPs varies depending on changes in chemical composition, microporosity, and pore size. These differences have been linked to the process of osteoinduction in-vivo. Research has highlighted the significance of the sintering process in controlling the pore size and porosity of CaPs, ultimately producing an osteoinductive ceramic material [50]. Despite their limitations in terms of mechanical properties such as strength and fatigue resistance, CaPs are commonly utilized as coatings and fillers rather than load-bearing materials. They are often applied as thin coatings on metallic implants to enhance bone fixation or as dense or porous blocks for bone grafts. Additionally, CaPs can be used in injectable compositions. Various custom-designed forms of CaPs, such as wedges for tibial opening osteotomy, cones for spine and knee applications, and inserts for vertebral cage fusion, are also available. CaPs find application in alveolar ridge augmentation, tooth replacement, maxillofacial reconstruction, orbital implants, hearing ossicle enhancement, spine fusion, and bone defect repair [51].

Among CaPs commonly reported for biomedical applications are HAp, α- and β-TCP, and biphasic CaPs (BCP), a mixture of HAp and TCP [46,52]. CaP and HAp have a chemical composition most similar to the inorganic section found in bone [53]. Despite its advantages, HAp has poor mechanical properties [54,55]. HAp can be synthesized using wet methods, including precipitation, hydrothermal synthesis, and solid-state reactions at temperatures above 1200 °C. These methods involve starting materials such as MCPM (monocalcium phosphate monohydrate), DCPA (dicalcium phosphate anhydrous), DCPD (dicalcium phosphate dihydrate), and OCP (octacalcium phosphate) [50,56,57]. TCP has a higher fracture toughness than HAp [58,59]. However, TCP is not a suitable bioceramic for load-bearing utilization due to its inferior mechanical strength compared to cortical bone [60]. Precisely, β-TCP is a high-temperature phase of CaPs obtained through thermal decomposition at temperatures exceeding 800 °C. There are three recognized polymorphs of TCP: β-TCP-stable below 1120 °C, α-TCP-stable between 1120 °C and 1470 °C, and α'-TCP, which is stable above 1470 °C. However, achieving densification of β-TCP can be challenging due to the low temperature of the β to α phase transformation, which limits the ability to sinter the material at high temperatures. Indeed, doping β-TCP with substances like magnesia or calcium pyrophosphate can stabilize the β to α phase transition at high temperatures. This modification allows for better densification of β-TCP at higher temperatures. β-TCP is a biodegradable material and has been extensively studied as a bone substitute. It can be used in various forms, such as granules or blocks and can also be incorporated into calcium phosphate-based bone cements. These applications make β-TCP a valuable material in bone tissue engineering and regenerative medicine [61]. In addition to the above-mentioned crystalline CaP materials, amorphous calcium phosphate (ACP) has attracted significant attention due to its variable physicochemical properties, excellent bioactivity, and superior biodegradation [62] as ACP performs as the precursor of the mineral phase of CaP and the storage pool of calcium and phosphorus, which regulates the formation and mechanical properties of bone [63]. Even though CaPs bioceramics include ideal bioactivity, they are fragile, with low impact resistance and fracture toughness [64]. TCP consists of four polymorphs, namely α, super-α, β, and γ. Despite having a higher fracture toughness than HAp, [58,59].

Cement based on calcium phosphates (CPCs) combines one or multiple calcium phosphates and a water-based solution. This mixture subsequently forms a less soluble calcium phosphate and solidifies by intertwining the developing crystals, giving the cement its mechanical rigidity. When applied to a bone defect, the paste solidifies on-site, at the body's temperature, and exhibits only limited solubility [65]. CPCs

possess several noteworthy characteristics, including exceptional biocompatibility and resorbability, bioactivity, non-cytotoxicity, the ability to promote the growth of osteoconductive pathways, and adequate compressive strength for various applications. CPCs demonstrate greater mechanical strength in compression than tension or shear due to the limited bonding between entangled crystals. Compressive strength values are typically 5–10 times higher than tensile strength. The main advantages of CPCs include their rapid-setting properties, excellent moldability, and ease of manipulation. As a result, these bioceramics are commonly used in filling bone defects and in trauma surgeries as moldable paste-like substitutes for bone materials. Additionally, like other bioceramics, CPCs offer the opportunity for bone grafting using alloplastic materials, which are readily available in unlimited quantities and do not pose the risk of infectious diseases [50].

2.4. Bioactive glasses (BGs)

BGs and glass-ceramics have been designed, in both porous and dense forms, for tissue engineering applications in dentistry and orthopedics. Heat treatment endows BG with improved toughness, strength, wear resistance, and elastic modulus [66,67]. BGs have demonstrated a faster ability to establish a bond with living bone tissue compared to other bioceramics. After implantation, they transform an apatite material. BGs release calcium (Ca), phosphorus (P), silicon (Si), and sodium (Na) ions upon dissolution, which can stimulate the osteogenic genes expression, angiogenesis, neovascularization, differentiation of mesenchymal stem cells (MSCs), and enzymatic activity [68–70]. BGs are non-cytotoxic and biocompatible materials [71], which are osteoconductive and can integrate with host bone tissue [67,72,73]. However, like many bioceramics, they suffer from poor mechanical characteristics [60,74]. CSs are also biocompatible and can be an appropriate candidate in tissue engineering applications due to their ideal bioactivity and biodegradability [75,76]. In addition to silicate glasses, the biomedical application of borate- and phosphate-based glasses was also reported [77,78]. Borate-based glasses have gained attention in biomedical applications due to their unique properties. These glasses typically comprise B_2O_3, Na_2O, CaO, and P_2O_5, exhibiting fast degradation rates. When immersed in an aqueous phosphate solution, borate-based glasses can completely convert into apatite, a mineral similar to the mineral phase found in bone. This conversion process is similar to that of Bioglass®, a well-known bioactive glass, but borate-based glasses do not form a silica-rich layer on the surface [77,78]. Borate glasses have indeed been used as drug-release systems for treating bone infection [79]. However, one disadvantage of borate glasses is the potential toxicity of boron. When the glass degrades, borate ions are released into the solution. In high concentrations, boron can be toxic to cells. However, this disadvantage can be mitigated in *in-vitro* dynamic culture conditions [80]. Phosphate bioactive glasses, with compositions in the Na_2O–CaO–P_2O_5 system, are known to have faster dissolution rates in aqueous fluids compared to silica glasses. This property can be advantageous in certain biomedical applications [81,82]. However, the fast degradation rate of phosphate glasses may not always be desirable, especially in applications where long-term stability is required. To address this issue, metal oxides such as TiO_2, Al_2O_3, and B_2O_3 can be incorporated into the composition of phosphate glasses. These metal oxides help stabilize the glass network, resulting in a slower degradation rate [83].

3. What are the various factors and approaches that can be implemented to enhance the mechanical durability of scaffolds?

3.1. Impact of scaffolds' structure on their mechanical characteristics

One of the factors involved in determining mechanical properties is porosity. For instance, HAp-scaffolds with 40–48 % porosity showed a compressive strength of about 25.30 MPa. With the increase in porosity from 70 % to 76.9 % and from 80.45 % to 91.4%, the compressive strength of the HAp-based scaffold decreases by 3.86 Mpa and 1.27 MPa (nonlinear), respectively. The correlation between porosity and compressive strength in the HAp with other bioceramics, HAp polymers, and TCP scaffolds can be observed [8]. The same relationship has also been reported previously. The compressive strength of HAp with other ceramic-based scaffolds nonlinearly decreased from 16.13 MPa to 2.31 MPa, with an increase in porosity from 54.62 % to 72.09 %. Finally, the decline was observed to 0.92 MPa when porosity reached 89.92 % [8]. However, in the TCP scaffold, the compressive strength exhibited a linear decline from 9.09 MPa to 0.65 MPa, with an increase of porosity from 50 % to 90 % [8]. This inverse relationship has been reported in other investigations [84,85]. However, this has not always been the case; according to a previous study, scaffolds based on HAp- Poly(methyl methacrylate))PMMA(showed a compressive strength of 7.26 $\pm$ 0.45 MPa (70 wt% HAp) with a porosity value of 75 $\pm$ 0.8 %, and this value increased when the porosity reached 71 $\pm$ 1.9 % (80 wt% HAp, compressive strength: 4.15 $\pm$ 29 MPa) [86]. The agglomeration of HAp particles was recognized because they were considered the weak point for the formation of microcracks [87]. Various factors such as powder particle size, materials, the manufacturing process, and sintering temperature can significantly affect bioceramic scaffolds' chemical properties and porosity [88].

A previous study reported a compressive strength of 27.4 $\pm$ 4.2 MPa for HAp scaffolds with only macroporosity (250–350 μm). When macroporosity of 2–8 μm was established in this HAp scaffold, the compressive strength increased to 34.4 $\pm$ 2.2 MPa [89]. Similarly, the crushing strength of Si-Ca-O ceramic scaffolds reduced from 23.7 $\pm$ 5.9–11.8 $\pm$ 4.1 MPa with increased pore size from 300 to 600 μm [90]. In another case study, compressive strength decreased from 40 MPa to 1.37 MPa by changing the average pore size of 20.5–458.78 μm (439–495 μm) [8]. On the contrary, Liu et al. reported a different relationship between compressive strength and pore size. Three HAp scaffolds with 400, 500, and 600 μm have been designed (stereolithographic 3D printing (SL-3DP)). Their compressive strength has been reported at 20.54 $\pm$ 4.53, 30.34 $\pm$ 4.07, and 38.48 $\pm$ 3.06 MPa, respectively. The compressive strength of the HAp scaffold increases proportionally with an increase in its pore size. Such results could be due to reduced manufacturing defects, as the number of pores decreases with larger pore sizes [91]. A previous study reported that change in the compressive strength of scaffold structures with pore sizes in the range of 200–400 μm is lower than other scaffolds with pore sizes lower than 200 μm or upper than 400 μm, which may be attributed to porosity as a reason. Therefore, regarding mechanical properties, particularly compressive strength, the overall porosity has a greater impact than the pore size. Different porosities were reported based on pore size. First: porosity of 48–68%, pore size lower than 200 μm; Second: porosity of 67–85 %, pore size exceeding 400 μm; The third value: porosity of 64–67%, pore size between 200 and 400 μm [8]. As the compressive strength of trabecular and cortical bones is announced at about 2–45 MPa and 90–230 MPa, respectively [92,93], many fabricated scaffolds with more than 40 % porosity can only be applied to substitutes for trabecular bone but are not ideal for the load-bearing utilizations. At the same time, scaffolds with higher compressive strength might be more appropriate for load-bearing applications and substitute for compact bones [94–96]. It has been reported that more than 90 % porosity is not preferable for bioceramics scaffolds, particularly for TCP bioceramics with a higher degradation rate. Since higher degradation decreases the mechanical properties and scaffolds' integrity before having adequate time for forming new bone [97].

In summary, the correlation between the compressive strength and porosity of BGs is shown in Fig. 2. Various compressive strengths can be achieved with 30–95% porosity. Overall, the compressive strength decreases with increases in the porosity percentage (Fig. 2b) [98].

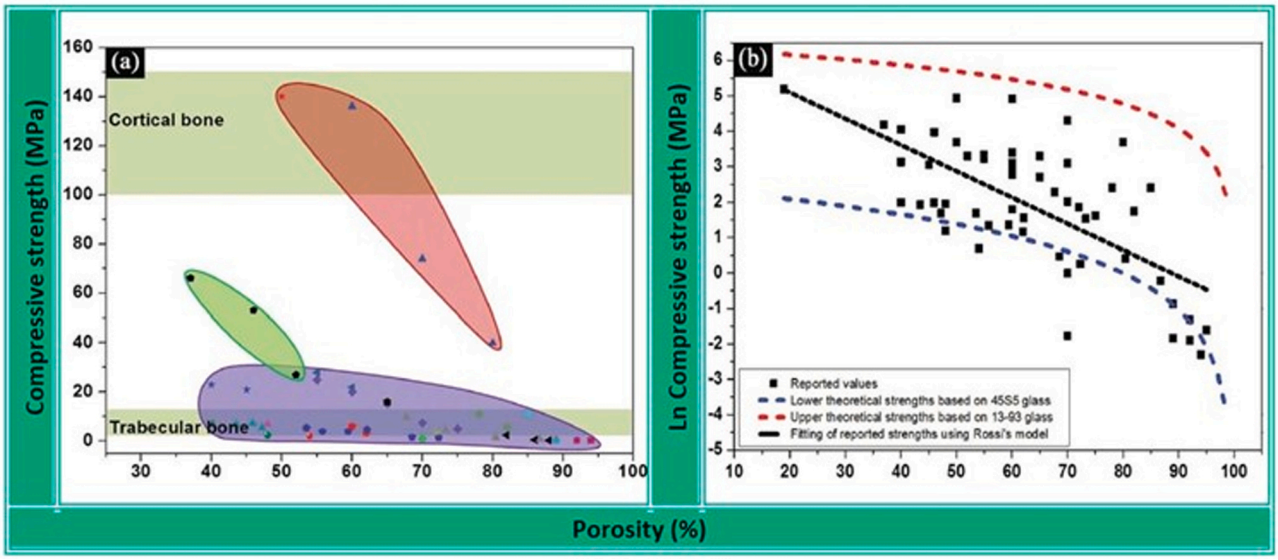

Fig. 2. The relationship between compressive strength and porosity in scaffold-based bioactive glasses [98] Figure reused from Fu et al., 2013 after license agreement 5271251292699. Copyright © 2013 WILEY-VCH Verlag GmbH & Co. KGaA, Weinheim.

3.2. Influence of the production method on scaffolds' mechanical properties

Various techniques have been developed to manufacture scaffolds. Available techniques can create an opportunity to ensure perfect control of the scaffolds' properties by using a computer for designing [98]. Some minimum requirements were considered necessary for good function and tissue ingrowth in the scaffolds, like structure and size of pores. Pores should be interconnected and larger than 100 μm [99]. Other factors necessary regarding the ingrowth of bone and mechanical features are neck shapes between closed pores and microporosity and the architecture of the solid phase [98].

3.2.1. Traditional methods

3.2.1.1. Foam replica. A previous study used the foam replica method to fabricate scaffolds from (13−93) BG. The scaffolds produced through the foam replica method could have a porosity of 85%, and the size of their pores could vary from 100 μm to 500 μm [99]. The compressive strength and elastic modulus were reported as 11 ± 1 MPa and 3.0 ± 0.5 GPa, in the order given [99]. Polyurethane foam is used to produce scaffolds, making a porous structure [100]. While a porous scaffold can be obtained via this method, the mechanical properties are a major limitation. Because the struts, which play a critical role in bearing mechanical forces, may be hollow, the overall strength of scaffolds is reduced [101,102]. Mesoporous bioactive glasses (MBGs) were initially produced by dipping polyurethane in a sol. However, a brittle structure was obtained with compressive strength in 50–250 kPa [103]. The replication technique has developed various strategies to enhance the foam's mechanical features. For instance, combining gel casting with the foam replication technique could enhance the mechanical features of HAp scaffolds [11,104–107].

3.2.1.2. Gel-casting foam. Another method has been suggested as an alternative to the foam replication method. The gel-casting foam method can also produce scaffolds [108]. Gel casting is generally applied to fabricate high mechanical-strength scaffolds with a low porous structure [109]. The primary advantage of this technique is that it enhances the mechanical characteristics of the scaffold compared to the foam replication method. In this method, the struts are not hollow. In a previous study, three different glasses– 13–93, ICIE16, and PSrBG – were used to produce scaffolds through the gel-casting foam method. Findings indicated that the mechanical qualities achieved were more robust than those of the scaffolds created through the foam replication process [110]. Compressive strengths of 15.3 ± 1.8 MPa, 8.4 ± 0.8 MPa, and 3.4 ± 0.3 MPa were observed for 13–93, PSrBG, and ICIE16, respectively [110]. Therefore, the factor affecting the mechanical properties is the fabrication method of scaffolds, as shown in this review using examples from previous studies.

3.2.1.3. Solvent casting. Solvent casting/particulate leaching is a conventional approach for manufacturing scaffolds. It starts by dissolving a polymer in an organic solvent. This method involves introducing porogens, substances that can be evenly distributed within a molded structure. Once the structure solidifies, these porogens are dissolved, leading to the formation of pores. Adding porogens to the polymer solution establishes a polymer-porogen network and contributes to the scaffold's structure. As the solvent evaporates, the polymer undergoes a hardening process. Following this, water is utilized to dissolve the porogen, commonly a salt like sodium chloride. This results in a polymer scaffold with a solid structure and a network of pores. However, it can be challenging to precisely regulate the shape and interconnectivity of the pores in scaffolds produced using this technique [17,111].

3.2.1.4. Freeze-drying. The freeze-drying technique, initially developed by Fukasawa et al. [112], is used to create porous ceramics. This technique utilizes material freezing in a specific direction, taking advantage of ice crystals to form columnar porous structures without the need for organic additives. Once the long and oriented ice crystals are formed, they are sublimated, followed by exposing the scaffold to high temperatures for consolidation [113]. The resulting scaffold exhibits excellent mechanical properties due to the oriented crystal structure. However, it should be noted that this process is both time-consuming and energy-intensive [114].

3.2.1.5. Comparing five different methods (solvent casting and salt leaching, gelate-freeze casting, freeze casting, a combination of sacrificial template and direct foaming, and replication). Different methods can impact the bioceramic scaffolds' mechanical characteristics. Jaafar et al. reported the impact of five methods on the compressive strength of β-TCP scaffolds, including solvent casting and salt leaching, gelate-freeze casting, freeze casting, a combination of sacrificial template and direct

foaming, and replication. The gelate-freeze casting method demonstrated the highest compressive strength compared to the combination of sacrificial template and direct foaming, freeze casting, solvent casting and salt leaching, and replication methods, which showed lower compressive strengths in descending order. The compressive strength of the scaffold was improved by using a method that created a cellular microstructure with smaller pores [115]. According to previous reports, the freeze-casting method decreased the scaffold's porosity due to the small size of the ice crystals. Using a pore agent in a gelate-freeze casting caused ice growth distortion, forming a cellular-like microstructure and increased porosity [116]. Scaffold fabricated by combining sacrificial template and direct foaming m Scaffold fabricated by combining sacrificial template and direct foaming method demonstrated marginally increased compressive strength than salt leaching and solvent casting. It was demonstrated that the porosity of the fabricated scaffold by these five methods and compressive strength varied from 30 % to 95 % and 0.4–5.0 MPa, respectively. It is interesting to note that increasing porosity resulted in a decrease in compressive strength. The gelate-freeze casting approach produces ceramic scaffolds that exhibit superior strength compared to alternative techniques. The compressive strength ranges from 1.81 MPa with a 40 % [117] porosity to 5.0 MPa with a 30 % porosity [107]. The porous scaffold's compressive strength was restricted when created through a sacrificial template and direct foaming. Other techniques, such as solvent casting, salt leaching, freeze casting, and replication, resulted in a 50–70 % porosity and a compressive strength of approximately 1–4 MPa [115]. In summary, each method used various solid concentrations, pore agents, preparation methods, templates, and processing parameters, which can affect the scaffold's porosity, morphology, and properties [118]. In this regard, Table 2 indicates an example for this section. The effects of three different methods (for the same material) on the mechanical properties have been shown.

3.2.2. Additive manufacturing

The bioglass scaffolds and active bioceramics made by traditional methods, such as gas foaming or foam replication, can hardly match the porosity parameters of cancellous bone [119,120]. Due to their inherent brittleness and poor strength, they can only be used in sites of the skeleton subjected to a minimal stress scale [121,122]. On the other hand, a porous scaffold can be created using additive manufacturing (AM) and has a unique external shape and porous internal microstructure [123]. The findings showed that the AM technology could perfectly match the scaffold to the problem areas and mimic the human tissue's normal tissue architecture [124,125]. Many AM processes are available, each with its unique way of depositing layers to create a part with different materials. Some methods involve materials melting or softening, such as selective lase melting (SLM), selective laser sintering (SLS), and fused deposition modeling (FDM). Meanwhile, other methods cure liquid materials like stereolithography (SLA). Direct energy deposition (DED) and laminated object manufacturing (LOM), in addition to those mentioned above, are introduced as the main AM methods [126].

There is growing consensus that 3D printing is a superior manufacturing technique to traditional methods due to its many advantages, including the ability to create complex geometry with high precision, significant material saving, design flexibility and customization [126]. With 3D printing, a wide range of ceramic, metallic, polymeric, and composite materials can be processed; nevertheless, choosing an ideal binder and optimizing process parameters is crucial for successful component creation. Various techniques and substances have been explored to enhance the mechanical characteristics of 3D printed ceramics structures compared to traditional techniques [127]. Similar to standard manufacturing technologies, the design of the process and the parameters used during the process heavily influence the characteristics of the product produced via AM (cost, the accuracy of the component, quality of the surface, mechanical and physical traits, etc.) as well as overall efficiency of the AM process [128]. Monshi et al. designed a bone scaffold from an electroconductive poly-lactic acid (EC-PLA) filament. Solid-work software was used to construct a scaffold model. The planned model was then transferred to a laminated, simplified 3D printer using its G-Code file to produce a scaffold with 65–75 % porosity. Cubic and cylindrical shapes were created and manufactured. HA nanoparticles were applied to increase the samples' chemical stability. The compressive strength of the designed structure has been reported 39.14 MPa. The obtained findings illustrated the adequacy of EC-PLA scaffolds' toughness and demonstrated that the EC-PLA scaffold is acceptable mechanically [129].

3.2.2.1. FDM. PLA is the most used material in the FDM method and can be combined with different elements, such as silver (Ag) or magnesium (Mg). During the preparation phase of a sample or model, FDM software enables modification of the density of the part or model by adjusting the infill percentage, which can have a major impact on mechanical properties, such as tensile strength. Some parameters are important to control as they can affect the mechanical properties such as layer thickness, printing head temperature, printing bed temperature, printing speed, infill percent, and infill shape [130]. For instance, it has been reported that the temperature of the nozzle affects the degree of the printed structure's crystallinity in the FDM technique. Elhattab et al. used a composite containing PLA and β-TCP to evaluate this effect. The results indicated that the nozzle temperature is directly proportional to the mechanical properties. When the nozzle temperature was set at 190 °C, the PLA and (β-TCP)-PLA samples displayed the lowest tensile strength with 65.8 (± 0.971) MPa and 54.344 (± 3.796) MPa, respectively. Conversely, when the nozzle temperature was set at 220 °C, both PLA and (β-TCP) -PLA samples showed better tensile strength with 75.77 (± 1.147) MPa and 69.711(± 6.23) MPa, respectively. These findings suggest that the mechanical properties of the printed samples improve as the nozzle temperature increases. In the same way, the results revealed that the lowest Young's modulus values were observed when the nozzle temperature was set at 190 °C with 1.725 (± 0.134) GPa and 1.685 (± 0.143) GPa for PLA and (β-TCP)-PLA, respectively. Conversely, the highest Young's modulus values were obtained when the nozzle temperature was set at 220 °C, with values of 1.837 (± 0.156) GPa and 2.161 (± 0.332) GPa for PLA and (β-TCP)-PLA, respectively [131].

3.2.2.2. SLS/SLM. SLS relies on high laser density, which combines ceramics, metals, or even polymers or composites to form a 3D end-product structure with exceptional mechanical properties and surface quality [130,132]. Like FDM, some parameters can affect the mechanical properties of products by the SLS method, including laser power, scan spacing, scan speed, etc. [133,134]. One can increase the laser power, scanning speed, hatch distance, and layer thickness to achieve a higher energy density. Such an increase in energy density can improve mechanical properties and higher part density, but only up to a certain point. It's important to note that further increases in energy density beyond that point may result in material degradation and a subsequent drop in both mechanical properties and dimensional accuracy [133]. The scan path should also be considered when SLS is used, as this can affect material shrinkage and manufacturing time. The scan path can determine the part's density and mechanical features consequently [135]. In addition, the print resolution, porosity, and mechanical properties can also be enhanced with powders with a consistent distribution of particle size and high density [136]. Selective laser melting (SLM) is a type of additive layer manufacturing (ALM) process that falls under the broader category of rapid prototyping/manufacturing (RP/RM) techniques [137]. SLM and SLS are recognized as one of the most versatile RM processes for creating intricate three-dimensional parts. In SLM, successive layers of powdered material are solidified by a laser, building up the final object layer by layer [138]. It's important to note that while SLS relies on a sintering mechanism to partially melt and

fuse the powder, SLM fully melts and fuses the powder material [139]. Hao et al. analyzed the performance and feasibility of SLM technique to directly manufacture a 316 L stainless steel /HAp composite. The objective was to create load-bearing and bioactive implants. Through the investigation, it was discovered that there is an optimal condition for fabricating high-quality 316 L stainless steel/HAp composite specimens using a duplicate scanning strategy during the SLM process. This finding suggests that the SLM technique can be effectively utilized for producing reliable and well-structured 316 L stainless steel /HAp composites. The 316 L stainless steel/HAp composite demonstrated a sufficient tensile strength of 95 MPa for load-bearing purposes. Moreover, it is not excessively rigid, which helps to avoid stress shielding [140].

3.2.2.3. Robocasting method. A polymer binder is applied in the robocasting method, and bioglass particles are dispersed throughout the binder [110]. For robocasting applications, the ink must possess shear-thinning rheology, allowing it to flow easily through a narrow nozzle when subjected to force. Additionally, the ink should retain its mechanical stability after extrusion and not deform while drying without causing cracks in the extruded filaments. Various factors, including the physical and chemical properties of the ink, the particle size of the glass, and the distribution of pores, influence the mechanical stability of the green body. Pluronic F-127, ethyl cellulose/polyethylene glycol, and carboxymethyl cellulose are commonly used polymeric binders for producing bioactive glass scaffolds through robocasting [141]. This method produces a porous structure with interconnected pores [142]. The diameter or width of at least 100 μm for interconnected pores and porosity of more than 50 % have been reported as requirements to allow tissue ingrowth in porous scaffolds. In addition, porosity can promote resorption, vascular ingrowth, osteoblast differentiation, and other bioactivities [143]. The properties of the fabricated scaffolds manufactured via robocasting methods are porosity of approximately 60 %, interconnection in the range of 100–500 μm, and compressive strength of roughly 136 ± 22 MPa [144].

Deliormanli et al. chose bioactive borate glass (13–93B3) and 13–93 BG [145]. Scaffolds were manufactured using the robocasting technique, and the final mechanical characteristics, other than pore sizes, of scaffolds based on different materials were evaluated. The overcomes of evaluations for compressive strength demonstrate 142 ± 20 MPa for 13–93 G, while the strength of 65 ± 11 MPa was reported for 13–93B3. The scaffolds had thick glass filaments with a 300 ± 20 μm diameter. They also contained interconnected pores approximately 420 ± 30 μm in width and had a porosity of around 50 %. (13−93)- and 45S5-BG scaffolds with mechanical characteristics close to the cortical bone have been produced using the 3D printing technique (direct link printing/robocasting) [145]. Liu et al. also fabricated the porous scaffold based on (13−93)-silicate glass by the robocasting technique. The prepared specimens were put at room temperature to dry, then heated (to 600 °C) and sintered (for 1 h, at 700 °C, in the air). Fabricated scaffolds had a pore height and width of 150 ± 10 μm and 300 ± 10 μm, in the order given. The compressive strength and elastic modulus were 86 ± 9 MPa and 13 ± 2 GPa, respectively, and these values were similar to the properties of cortical bone (Elastic modulus: 10–20 GPa, compressive strength: 100–150 MPa). The mentioned compressive strength falls towards the lower reported values for human cortical bone [146]. Liu et al. conducted a study where they utilized robocasting techniques to create grid-like porous scaffolds using a 13–93 silicate glass composition (53SiO2, 6Na2O, 12K2O, 5MgO, 20CaO, 4P2O5 wt%) as the material. Following the printing process, the samples were dried in air at room temperature for one day, then heated to 600 °C in an oxygen environment to remove processing additives. Subsequently, the scaffolds were sintered in air for 1 h at 700 °C. The resulting scaffolds exhibited a grid-like microstructure, with a pore width of 300 ± 10 μm in the deposition plane (xy plane) and a pore height of 150 ± 10 μm in the direction of deposition (Z-axis). The scaffolds' flexural strength and flexural modulus were measured to be 11 ± 3 MPa and 13 ± 2 GPa, respectively, which falls within the lower range of values for trabecular bone. Furthermore, the compressive strength and compressive modulus were 86 ± 9 MPa and 13 ± 2 GPa, respectively, which closely resemble values typically found in cortical bone [146].

3.2.2.4. Introduction of AM processes for fabrication of high-performance ceramics (HPC). Several AM processes have been introduced to fabricate high-performance ceramics (HPC), including (i) binder jetting (BJ), (ii) vat photopolymerization (VP), (iii) material extrusion (ME), (iv) material jetting (MJ), (v) sheet lamination (SL), (vi) powder bed fusion (PBF), and (vii) directed energy deposition (DED). As AM expands, it enables the production of functional parts without additional tools or processing, reducing lead time. However, it remains uncertain whether the mechanical properties of AM-produced parts meet the same standards as those produced through traditional methods like sand casting, roll-forming, and injection molding. Although most materials' flexural strength and fracture toughness values are comparable to AM and traditional methods, conventional zirconia manufacturing can achieve higher flexural strength values. Nevertheless, the VP process can produce high-density and low-porosity oxide materials. In addition, the VP process enables the production of intricate structures with extreme overhangs and small shells without the risk of crack formation. However, the LOM process may compromise the flexural strength of aluminum nitride manufactured via the AM method, which generally results in high-resolution layers but poor inter-layer bonding. While not all HPC materials have been utilized to create functional materials, nitrides and carbides are often the focus of research [147]. Table 1 shows some benefits and drawbacks of AM techniques.

In summary, traditional methods, such as gel-casting foam etc., have

Table 1
Some main advantages and disadvantages of main AM's methods [127].

Method	Advantages	Disadvantages
Fused deposition modeling (FDM) [148,149]	• Low cost • High-speed • Simple to execute	• **Weak mechanical properties** • Poor surface quality • Limited used materials
Powder bed fusion	• High-quality in printing • Fine resolution • Powder ben can act as support for the printed objects	• The process can be slow • High cost • Risk of **high porosity** when the powder is fused with a binder
Laminated object manufacturing	• **Using a broad range of materials, including ceramics** • Low cost • Reduced manufacture time	• Difficulty in manufacturing complex shape
Direct energy deposition	• **Great mechanical properties** • **Polymer-ceramics can be used** • Microstructure can be controlled	• Difficulty in manufacturing complex shapes with details • Surface quality is low • Accuracy is low
Stereolithography	• Good resolution • Good quality	• Limited materials can be used • Expensive • The speed of printing is slow
Inkjet printing and contour crafting	• **Ceramics can be used** • Large structures can be printed	• Inadequate adhesion between layers • Resolution can be coarse
SLS[150]	• **High mechanical features** • Ceramics, polymers, and metals can be used	• Low speed • High cost
SLM[150]	• **High mechanical features** • High speed	• Limited materials • High cost

Table 2
The effect of different methods and materials on the mechanical properties.

Materials	Methods	Porosity %	Compressive strength (MPa)	Reference
Same material and different manufacturing methods				
13–93	Replica	85 ± 2	11 ± 1	[12]
13–93	Gel casting	75.4 ± 2.1	15.3 ± 1.8	[14]
13–93	Robocasting	50	142 ± 20	[145]
Same manufacturing methods with different materials and sintering procedure				
13–93	Gel casting	75.4 ± 2.1	15.3 ± 1.8	[14]
PSrBG[#]	Gel casting	76.7 ± 0.9	8.4 ± 0.8	
ICIE16[*]	Gel casting	74.9 ± 1.3	3.4 ± 0.3	

[#] PSrBG: (44.5-mol% SiO_2, 4.5-mol% P_2O_5, 17.8-mol% CaO, 4-mol% Na_2O, 4-mol% K_2O, 7.5-mol% MgO, 17.8-mol% SrO)

[*] ICIE16: (49.46-mol% SiO_2, 1.07-mol% P_2O_5, 36.6-mol% CaO, 6.6-mol% Na_2O, 6.6-mol% K_2O)

been used to create scaffolds from bioactive ceramics and glasses. However, these techniques often lead to irregular pore geometries, resulting in regions with low pore interconnectivity, which compromises bioactivity, and high-stress concentration under load, which compromises mechanical properties. 3D printing, on the other hand, addresses these issues by allowing for precise control of pore geometries. For bioactive glasses and ceramics, commonly used 3D printing methods include extrusion-based robocasting, SLA, selective laser sintering, etc. [151]. The novel Am methods can control multiple parameters during the process. The structure and materials should be considered to optimize each method's characteristics and parameters. The number of research on the production of bioceramic scaffolds by AM is expected to be more than the current one, which can overcome this method's limitations and make scaffolds with sufficient mechanical properties and promising bioactivities.

3.3. Impact of parameters used in the manufacturing method on the mechanical characteristics of scaffolds

3.3.1. Impacts of cooling rate

The cooling rate was another parameter affecting compressive strength. Maximum compressive strength was achieved by enhancing the cooling rate [152]. Sarkar et al. designed scaffolds in which the freeze-casting method was used in its producing process from nano-HAp and gelatine and showed that the compressive strength improved when liquid nitrogen was applied for curing; however, increasing the curing time decreased the scaffolds' strength. Thus, the curing time and the solutions used for additional treatment are the other factors that can influence mechanical properties [153]. In addition, Müller et al. reported other conditions that may affect the mechanical properties of titanium oxide (TiO_2) scaffolds, including grain boundary and the cooling rate. Finally, it was observed that increasing the cooling rate and fasting can prevent or decrease the creation of grain boundary impurities, and consequently, the compressive strength increased [154]. Hafezi et al. investigated the impact of cooling rate on the mechanical properties of calcium zirconium silicate (Ca3ZrSi2O9 or Baghdadite)-based scaffolds fabricated by water-based freeze casting technique. As the cooling rate increased while keeping the solid loading constant, the linear shrinkage and porosity parameters decreased, and strength significantly increased.

Based on the mechanical results, the scaffold exhibited the best mechanical properties when prepared with a cooling rate of 4 ℃/min. Scaffolds produced with a freezing rate of 1 ℃/min (solid loading: 20 % (v)) exhibited compressive strengths of 1.8 MPa, and elastic moduli of 41.3 MPa, respectively. In contrast, scaffolds frozen at a rate of 4 ℃/min (solid loading: 20 % (v)) displayed a higher compressive strength of 2.1 MPa and an elastic modulus of 59.8 MPa. This improvement in microstructure enhanced both the compressive strength and elastic modulus of the scaffolds [155]. Farhangdoust et al. also announced that as the cooling rate increased, the compressive strength of the ceramic bodies (macroporous hydroxyapatite scaffolds) consistently increased while the lamellar space decreased. Specifically, the compressive strengths were measured as 4.1 MPa, 6.4 MPa, and 9.5 MPa at cooling rates of 2 °C/min, 8 °C/min, and 14 °C/min, respectively. The increased cooling rate led to larger temperature gradients, resulting in smaller pore sizes. Consequently, the strength of the ceramic bodies increased [88].

In conclusion, as some studies have been reviewed in this section, it can be found that the cooling rate is one of the effective parameters in improving the mechanical properties of bioceramics scaffolds. Since the cooling rate increases, the compressive strength of ceramics can improve.

3.3.2. Impact of sintering time and temperature

Factors other than the method can also have effects on mechanical features. Deville et al. [152] investigated these factors in fabricating scaffolds based on HAp using freeze casting. It was shown that the process conditions are also influential. In particular, the results showed that sintering is one of the influential conditions. As a result, the compressive strength was enhanced, and porosity was reduced with increases in sintering temperature. The impact of the sintering time and the recoating process on the mechanical properties was also evaluated previously. Enhancing the sintering time (more than five hours) improved the mechanical properties. Furthermore, the recoating considerably improved the ceramics' structure [156]. It has been reported that using some glass in the main components can be a sintering aid or enhance the sintering temperature. For instance, the previous study fabricated scaffolds containing a mix of 45S5 BG and calcium borosilicate glass-derived sol-gel. Specimens were sintered at a range temperature from 800° to 1000 °C for 2 h. According to the findings, utilizing 10 % calcium borosilicate in BG material and sintering it within the 850–900 °C temperature resulted in significantly higher compressive strength than those sintered at lower or higher temperatures. The strength observed was approximately 2.5–3 times more than that of the 45S5 BG material without calcium borosilicate. The porosity levels were slightly lower at 850 °C and 900 °C (approximately 70.4 %−72.8 %) compared to those sintered at 800 °C (which had a porosity of 76.4 %). However, at a sintering temperature of 1000 °C, there was a significant decrease in porosity from the samples treated at 900 °C. This decrease may be attributed to better densification of the BG struts at higher sintering temperatures. In the meantime, the compressive strength improved with temperature, reaching over 7.3 MPa at 850 and 900 °C, considerably more excessive than that sintered at 800 °C (<4.1 MPa) [35]. Eom et al. also reported how the mechanical characteristics of porous silicon carbide are affected by variations in sintering temperature. The study revealed that as the sintering temperature increased from 1800 °C to 1950 °C, there was a significant improvement in both compressive strength (from 50 MPa to 100 MPa) and flexural strength (from 50 MPa to 290 MPa) [157]. A previous study designed biomimetic scaffolds containing HAp, TCP, and CS to investigate the effects of sintering temperature on mechanical features. The result showed that with the increase of sintering temperature from 1050 ℃ to 1250 ℃, porosity reduced from 63.7 % to 47.1 %. The flexural strength increased from an initial value of 4.9 ± 0.06 MPa to a final value of 38.5 ± 0.44 MPa, while the flexural modulus increased from an initial value of 1.05 ± 0.02 Gpa to a final value of 3.08 ± 0.02 GPa [158]. Perera et al. also reported that increasing the sintering temperature (1100–1200 ℃) enhanced the strength. The initial value of 36.5 ± 0.4 MPa reached 46.3 ± 0.4 MPa for the β-TCP specimens. The 1200 ℃ (for 3 h) was a temperature that obtained optimal performance [159]. Similar results were observed for the natural HAp that increasing sintering temperature increased mechanical properties [160]. Other investigations also

characterized the impact of sintering temperature on the mechanical characteristics and reported that this could be a prominent factor in regulating the mechanical features of scaffolds [55,161,162]. For example, HE et al. An analysis was conducted on various elements involved in the manufacturing process of bioceramic scaffolds made from HAp, specifically through the implementation of digital light processing (DLP), which utilizes additive manufacturing techniques. When the solid loading was set at 50 vol%, the flexural strength initially increased and then decreased as the sintering temperature increased (sintered at 1200, 1250, and 1300 ℃ flexural strength were 12.9, 18.3, and 12.1 Mpa). On the other hand, the compression strength consistently increased with the increase in sintering temperature (sintering temperature of 1200, 1250, and 1300 ℃: compression strengths of 12.5 ± 7.5, 16.9 ± 6.8, 18.1 ± 7.1 MPa were reported, in order).

According to the results, increasing sintering temperature enhanced compression strength [163]. However, it is not always the case that increasing the sintering temperature enhances the strength. Liao et al. demonstrated this by creating bioceramic scaffolds with inter-porous structures using different fabrication temperatures ranging from 900° to 1500 °C. They utilized a customized 3D printer that employed a laser-assisted gelling (LAG) process to manufacture the scaffolds, which were constructed from raw materials such as CaCO3 and SiO2. $CaCO_3$ powder was introduced into the SiO_2 mixture as separate additions to enhance mechanical properties, with 5 wt% and 9 wt% [164]. The different scaffolds fabricated were sintered at varying temperatures, ranging from 900° to 1500 °C, and their mechanical properties were subsequently analyzed. The scaffolds exhibited favorable properties when the composite ratio of CaCO3:SiO2 was 5: 95, and the sintering temperature was 1300 °C. At these conditions, the compressive strength of the scaffolds was measured to be 47 MPa, and the porosity was found to be 34 %, which indicates that the scaffolds had good mechanical properties and an appropriate porosity for potential biomedical applications [163]. When the heat treatment temperature was increased to 1500 °C, the strengths of both scaffolds with CaCO3:SiO2 ratios of 5:95 and 9:91, respectively, were significantly reduced. In summary, the sintering temperature significantly influences the mechanical properties and strength of porous ceramics. Moreover, in most studies, higher sintering temperatures tend to enhance the mechanical properties, but there have been some reversed results mentioned in this section.

3.3.3. Impact of solid loading

Previously, the effect of solid loading has been investigated on the calcium zirconium silicate (Ca3ZrSi2O9 or Baghdadite)-based scaffolds by Hafezi et al. By manipulating the solid loading and cooling rate (which was reviewed in Section 3.3.1), various structures with varying pore sizes and strength characteristics were achieved. The study focused on examining the impact of cooling rate and solid loading on the scaffolds' pore sizes and mechanical properties. Increasing the solid loading from 12.5 % to 20 % (v) resulted in a reduction in porosity and an increase in compressive strength for both cooling rates. Scaffolds produced with a freezing rate of 1 ℃/min and solid loading of 12.5 % (v) exhibited compressive strengths of 1.3 MPa and elastic moduli of 26.2 MPa, respectively. With increasing the solid loading to 20% (v) at the same cooling rate, compressive strengths of 1.8 MPa and elastic moduli of 41.3 MPa were obtained, respectively. Scaffolds produced with a freezing rate of 4 ℃/min and solid loading of 12.5 % (v) exhibited compressive strengths of 1.5 MPa and elastic moduli of 21.8 MPa in order. With increasing the solid loading to 20 % (v) at the same cooling rate, compressive strengths of 2.1 MPa and elastic moduli of 59.8 MPa were obtained, respectively [155]. Also, the effect of solid loading in another study has been investigated. It has been reported that a higher solid loading is necessary to achieve the highest relative density and mechanical properties in HA-resin slurries. The possible explanation is that low solid loading can lead to significant shrinkage deformation, cracks, and defects during the binder removal and sintering process. The obtained results were as follows:

- solid loading 40 vol% and sintering temperature of 1200, 1250, and 1300 ℃: Compression strengths of 9.3 ± 4.4, 13.0 ± 3.3, 14.5 ± 4.2 MPa were reported, respectively.
- solid loading 45 vol% and sintering temperature of 1200, 1250, and 1300 ℃: Compression strengths of 12.0 ± 4.6, 15.9 ± 3.7, and 21.4 ± 5.1 MPa were obtained, respectively
- solid loading 50 vol% and sintering temperature of 1200, 1250, and 1300 ℃: Compression strengths of 12.5 ± 7.5, 16.9 ± 6.8, 18.1 ± 7.1 MPa were reported, in order.

The compression strength of HAp bioceramics was observed to increase with an increase in solid loading because the density of the ceramics also increases as more solid is added [163]. Lee et al. also reported the same results that the sintered body (porous mullite–alumina composite), which had a solid loading of 40 wt% and was sintered at 1500 °C, demonstrated the highest compressive strength of approximately 64.3 MPa. Additionally, it had the lowest porosity of 61.2 %. This compressive strength value was approximately three times higher than that obtained after sintering at 1500 °C (solid loading of 20 wt%) [165].

In conclusion, it is noteworthy that solid loading, sintering temperature, and cooling rate are influential and can affect the mechanical properties. These parameters should be controlled carefully during the process to fabricate a targeted scaffold with desirable properties.

3.4. The effects of bioceramics materials construction on the mechanical features of scaffold

The selection and use of materials for preparing scaffolds also affect the mechanical properties (Table 1 indicates the impact of three different materials fabricated with the same manufacturing method, for example). For instance, surfactant concentration produced an interconnected structure and pores. For all composition-based glass types, the concentration of Triton X-100 surfactant ranged from 0.2 to 0.06 ml. It has been reported that increasing the surfactant amount led to improved pores' sphericity and homogeneity. However, it also decreased compressive strength [110]. An essential factor in the selection of materials is their particle size. The effect of nanoparticles has been evaluated [166,167], and some examples are reviewed in the following section.

3.4.1. Glass-ceramics

With thermal treatment and high-temperature application, BGs can crystallize. This structure increases glass-ceramics' strength and creates glass-ceramics with more outstanding toughness than glass [141]. Table 3 shows that it is possible to compare different BGs and glass-ceramics. For instance, the glass-ceramic variety of Cerabone apatite wollastonite (AW) has more robust mechanical qualities than 45S5BG and HAp. Thus, AW glass-ceramics can replace vertebrae, where considerable compressive strength is required [168]. However, the bioactivity of glasses decreases with crystallization, as the bioactivity and ion exchange between glasses and the host tissue depends entirely on the presence of the glass phase. Hench et al. announced that the bioactivity of 45S5BG was not affected if the crystalline phase was under approximately 40 % [169].

The mechanical features of glass-ceramics containing magnesium (Mg) have also been investigated previously. In the $CaO\text{-}P_2O_5\text{-}MgO\text{-}SiO_2$ system, the increase of P_2O_5 content led to reduced compressive strength [170]. In another system with MgO and MgF_2, the thermal and mechanical analysis were evaluated with different contents of MgO (4, 25, and 46 wt%). Higher MgO content led to a higher endothermal peak (from 278, 697, and 950 °C at 4 % of MgO to 299, 736 and 990 °C at 46 % of MgO), which was applied in the sintering process. After sintering, increased MgO content enhanced the microhardness (from 5192 ± 5.3 % to 6467 ± 5.9 % MPa) and bending strength (211–280 MPa) of $CaO\text{-}P_2O_5\text{-}MgO—MgF_2\text{-}CaF_2\text{-}SiO_2$ glass-ceramic [171]. Previously,

Table 3
The mechanical properties of bone and different materials (glass, ceramics, and glass-ceramics) [122,141,179–181].

Materials	Compressive strength (MPa)	Bending strength (MPa)	Compressive modulus (GPa)	Vickers hardness (MPa)
Glass				
45S5 bioglass	—	40	60	—
52S4.6 bioglass[&]	—	40	60	—
Ceramic				
Hydroxyapatite	100–150	60–120	35–120	90–140
Glass-ceramic				
Cerabone apatite wollastonite	1080	215	120	680
Ceravital	500	100–150	100–160	—
Bioverit I (Apatite and fluorphlogopite)	500	140–180	70–90	—
Bioverit II (Apatite and fluorphlogopite)	450	90–140	–	–
Bone				
Cortical bone	100–135	50–150	7–30	60–75
Trabecular bone	1.5–7.5	10–20	0.05–0.6	40–60

&, 52S4.6 bioglass: (52.1-mol% SiO_2, 23.8-mol% CaO, 21.5-mol% Na_2O, 2.6-mol% P_2O_5).

research revealed the positive effects of adding 0.2 wt% Y_2O_3 to bioactive MgO-CaO-P_2O_5- SiO_2-CaF_2 glass. This addition resulted in glass-ceramic samples that exhibited enhanced hardness, fracture toughness, and compressive strength compared to the original glass. However, it was also observed that the addition of Y2O3 had a detrimental impact on the bioactivity of the parent glass [172].

Generally, BG implants should contain sufficient and appropriate mechanical properties to match soft and hard tissue [141]. Arepalli et al. also found that adding strontium (Sr) to the composition increased the bulk, Young's, and shear moduli (Elastic moduli) of BGs [173]. The incorporation of 5 wt% of copper (Cu) or lanthanum (La) also has some effects on the mechanical features of sol-gel glass scaffolds (67 % SiO_2–5 % Na_2O-24 % CaO – 4 % P_2O_5, mol%). La had a (7–18 %) improvement in compressive strength, but Cu caused an increase of about 221% more than pure glass [174]. Bachar et al. investigated the impact of fluorine and nitrogen on the mechanical properties of two bioactive glasses. In order to improve their mechanical characteristics, two groups of bioactive glasses were subjected to nitrogen doping. The first group, series (I), consisted of bioglass compositions without P_2O_5 within the SiO_2-Na_2O-CaO-Si_3N_4 quaternary system. The second group, series (II), involved substituting CaO with CaF_2 in the glasses from series (I) while maintaining a constant Na:Ca ratio. The addition of nitrogen in the bioactive glasses resulted in a linear increase in density, glass transition temperature, hardness, and elastic modulus. Such evidence suggests nitrogen incorporation strengthens the glass network, as nitrogen primarily forms 3-fold coordination with silicon atoms.

On the other hand, introducing fluorine led to a significant decrease in thermal property values but did not impact the mechanical properties of the glasses. When nitrogen and fluorine were combined in oxy-fluoronitride glasses, better mechanical properties were achieved at lower melting temperatures. This is because fluorine reduces the melting point, allowing for higher nitrogen solubility while maintaining the improved mechanical properties of nitrogen incorporation. The microhardness of the glasses showed an increase in nitrogen content. For the glass series containing nitrogen, the microhardness increased from 5.37 $\pm$ 0.2 GPa for 0 at% nitrogen to 6.27 $\pm$ 0.3 GPa, representing a 15 % increase at 3.3 at% nitrogen. Similarly, in the glass series containing nitrogen and fluorine, the microhardness increased to 6.77 $\pm$ 0.1 GPa, a 24 % increase, at 4.5 at% nitrogen [175]. Also, high-strength bioactive ceramics were developed by adding zirconia to a MgO-CaO-SiO_2-P_2O_5 glass-ceramic system, sintering, and hot isostatic pressing. The resulting bioceramic material displayed exceptional mechanical properties, including a bending strength ranging from 400 to 1000 MPa and a fracture toughness ranging from 3 to 5 MPa.$m^{1/2}$. These impressive properties were achieved by incorporating 30–80 vol% of zirconia into the ceramic matrix [72,176]. According to Zue et al., adding zirconia to mesoporous bioactive glass scaffolds resulted in several beneficial effects. Firstly, it enhanced the compressive strength of the scaffolds, making them more robust. Secondly, it reduced the dissolution rate of the scaffolds, leading to improved stability. Additionally, the incorporation of zirconia helped maintain a more stable pH environment within the scaffolds. Lastly, the scaffolds retained their ability to form apatite, which is important for promoting bone regeneration.

Generally, glass-ceramics containing zirconia exhibit a high fracture toughness due to the tetragonal-monoclinic transformation within the material. This transformation helps to absorb and dissipate energy, making the glass-ceramics more resistant to fracture [177]. Research has been conducted to examine the impact of incorporating CuO on the mechanical properties and in-vitro cytocompatibility of a glass-based scaffold derived from the 1393 bioactive glass composition. The general formula of the scaffold is (54.6 − X)SiO_2·6Na_2O·7.9 K_2O·7.7 MgO·22 CaO·1.74 P_2O_5·XCuO, where X represents the mole percentage of CuO and can take values of 0, 1, 2, or 3. The compressive strength of the 1393 scaffold was determined to be 6.9 MPa. However, when CuO was incorporated into the scaffold at different mole percentages (1, 2, and 3 mol%), the compressive strengths increased to 7.1, 7.3, and 7.6 MPa, respectively [178]. Several studies have explored the BG scaffolds' mechanical properties; hence, the mechanical properties of different materials have been shown in Table 3.

A previous study reported that using nano-size bioceramics significantly affected the mechanical properties compared to the micro size. The bioceramic scaffolds made from the nano-size powder of b-tricalcium phosphate [β-$Ca_3(PO_4)_2$, β-TCP] have a 10.87 MPa compressive strength. It was about twice as many as the micro-size scaffolds produced. The porosity levels were approximately 65 %, with uniformly distributed 400–550 micrometers macropores. Additionally, the interconnected pore size was around 100 micrometers [182].

3.4.2. Silicate-based ceramics

Si can be a prominent element in human bone and bone growth. Regarding the bone growth process, Si has a direct role in the mineralization of bone. A mix of extracellular matrix and bone matrix contains approximately 100–250 ppm Si level [183]. As Si is important in the body, various Si bioceramics have been developed and researched [141]. The preparation method of these types of bioceramics also affects the mechanical properties. Different methods, such as sol-gel [184], solid reaction technique, hydrothermal technique, and the precipitation of chemicals, are applied in synthesizing Si-based bioceramics [185–188]. Compared to HAp, Si-based bioceramics, including monticellite, hardystonite, dicalcium silicate, and wollastonite, have more excellent fracture toughness and bending strength [186]. However, some Si-based bioceramics have better mechanical properties than wollastonite and dicalcium silicate [189]. Notably, $CaSiO_3$ includes a quick rate of formation and a good level of apatite development in the simulated body fluid (SBF) solution [190]. However, its mechanical features are poor. It is challenging to shape and build porous structures with $CaSiO_3$, making it difficult to create $CaSiO_3$ scaffolds with uniform pore sizes and structures, controllable porosity, and appropriate mechanical strength [191]. It has been investigated that the problem of mechanical properties can be solved by combining $CaSiO_3$ with forsterite Mg_2SiO_4. The higher the Mg_2SiO_4 ratio in composites, the greater the improvement in their bending strength. Specifically, the bending strength increased from 35.1 $\pm$ 2.0 MPa (observed in composites containing 100 % $CaSiO_3$) to 168.4 MPa when the composite ratio consisted of 70 % Mg_2SiO_4. Also, Young's modulus of 17.3 $\pm$ 1.2 MPa and 22.3 $\pm$ 7.2 MPa have been reported for $CaSiO_3$ and 70 % Mg_2SiO_4 composite ratio, respectively [190]. The forsterite Mg_2SiO_4 has insufficient

mechanical features compared to the cortical bone, and it is impossible to use it for some applications [141]. Thus, researchers have tried to find a solution and develop materials, such as nanostructures, based on forsterite bioceramics. Webster et al. invented the first group of nano-sized ceramics [192]. Peng et al. applied graphene to develop the mechanical properties of $CaSiO_3$. $CaSiO_3$'s compressive strength reached 42.45 ± 4.30 MPa by adding 0.5 wt% graphenes, which was about 142 % more than pure $CaSiO_3$. Nevertheless, it was reported that adding more than 0.5 wt% (1.0, 2.0 wt%) decreased compressive strength (34.89 ± 3.78 MPa and 25.34 ± 1.66 MPa, respectively) [143]. Adding Nano-Zirconia (nano-ZrO_2) is an effective approach for enhancing the mechanical properties of $CaSiO_3$. Compressive strength enhanced from 17.9 MPa to 44.1 MPa, incorporating 40 % (wt%) of nano-ZrO_2 [193]. As a new kind of bioceramics, Akermanite has been introduced as a reinforcement to CS and CaPs nanopowders to boost their biomechanical properties. Joneidi Yekta et al. investigated the impact of adding non-toxic magnetite nanoparticles (0 %, 5 %, 10 %, and 15 % (wt%)) into a $CaSiO_3$ scaffold containing akermanite powder fabricated by the space holder method, followed with one hour sintering at 1100 °C. The Young's Modulus were reported 60 ± 5, 85 ± 5, 110 ± 5, and 145 ± 5 MPa in samples with magnetite nanoparticle of 0 %, 5 %, 10 %, and 15 %, in order [194].

3.4.3. Hydroxyapatite (HAp)

HAp can be considered the primary material and component for bone and jaw applications [195]. Specific characteristics of HAp, like mechanical properties and bioactivities, allow it to be used extensively for different purposes [19]. A similar strategy is to combine HAp with other polymers. Poly (lactic acid) (PLA)-HAp scaffolds had a better mechanical strength than HAp scaffolds fabricated by electrospinning. The previous study reviewed the combination of PLA with ceramics [196]. Padmanabhan et al. used wollastonite in the HAp composition to reinforce the mechanical properties. The specimens containing 50 %– 50 % HAp and wollastonite fabricated by foam replica showed the highest compressive strength (1.02 ± 0.16 MPa), higher than pure HAp scaffolds (0.51 ± 0.14 MPa) [197]. Wei et al. also designed a composition to enhance the mechanical features of a 3D-printed HAp bone scaffold. This research employed a method of incorporating carboxymethyl chitosan (CMCS) into HAp scaffolds through physical blending. Piezoelectric inkjet 3D printing was used to manufacture ceramic scaffolds composed of a composite material consisting of HAp and CMCS. The compressive strength and elastic modulus of specimens enhanced considerably with the enhancement of CMCS content. The compressive strength was announced to be 3.74 ± 0.2 MPa for pure HAp specimen. The strength of this material was slightly lower than that of cancellous bone in humans, ranging from 4 to 12 megapascals (MPa). Additionally, the elastic modulus of this material was 89.7 ± 11.3 MPa, which was significantly less than the elastic modulus of human cancellous bone, which typically ranges from 100 to 500 MPa. Regarding HAp/CMCS specimen containing 1 wt% CMCS, the elastic modulus and compressive strength were 148.4 ± 15.7 MPa and 4.71 ± 0.2 MPa, in order. Although these mechanical properties obtained were only within the mechanical range of cancellous bone, the overall level was still low. When the content of CMCS in the composite powder was increased to 3 wt%, the resulting compressive strength and elastic modulus were measured at 7.75 ± 0.5 MPa and 249.3 ± 17.1 MPa, respectively. These values represent an increase of 2–3 times compared to a pure HAp specimen. Thus, by enhancement of CMCS' content, the compressive strength and elastic modulus become higher [198]. Recently, Xiangfeng et al. reviewed the impact of the pore size of CaPs ceramics on their mechanical features. Investigations demonstrated that it is required to decrease their grain size to improve the mechanical properties of HAp and HAp/TCP bioceramics. For example, Vickers hardness of 9.5 and 4.86 GPa have been reported for HAp composition with average grain sizes of 700 and 193 nm, respectively [199]. Also, combining bioceramics with other materials has been introduced as another strategy to boost their mechanical properties [200,201]. According to Asa'ad et al., poly(lactic-co-glycolic) acid (PLGA) is a well-known polymer in tissue engineering due to its ability to maintain mechanical stability and low degradation rate. However, its major disadvantage (like a lack of inherent bioactivity) might be solved by adding HAp in composition to create bioactive interfaces. The combination of PLGA (about 10 %) and the 3D-printed HAp scaffold (90% in weight) illustrated good absorbent capacity and elastic characteristics [202–205]. Additionally, using natural and synthetic zeolites has been reported as another solution to overcome the mechanical weakness of HA. Zeolites refer to micro-permeable, hydrated tekto-alumina silicates made up of 3D structures of SiO_4 and AlO_4, which are tetrahedral and linked together via oxygen atoms. Clinoptilolite (Cpt, $(Na, K)_6(Al_6Si_3O)O_{72}{\cdot}nH_2O$)) is a significant type of natural zeolite. Alshemary et al. created 3D porous scaffolds consisting of Cpt-HA composites using polyethylene glycol (PEG) and polyvinyl alcohol (PVA) as porogen. According to mechanical evaluations, incorporating a large amount of Cpt (=2.0 g) caused a composition with high compressive strength (34.77 MPa) and 64 % porosity [206]. However, some studies showed that the combination of bioceramics has a negative impact on mechanical properties. Evis et al. proved this point by combining boron-doped HA-baghdadite (0, 5, 10, 15, and 20 (wt%) to design a 3D porous bioceramics. With the increase of baghdadite amount (0–20%), the compressive strength decreased from 15.05 ± 1.29–6.78 ± 0.39 MPa. Intriguingly, the content of baghdadite did not have any impact on tensile strength [207].

3.5. Effect of nanoparticle on the mechanical properties

3.5.1. Nano hydroxyapatite (nHAp)

The nHAp in different concentrations (5, 10 wt%) were applied by Abdal-hay et al. in composition to fabricate scaffolds. The nanoplates increased the specimens' Young's modulus and tensile strength [208]. The one case study applied the nanocomposites of HAp and PCL as a coat for scaffolds based on BCP; the coated specimens' compressive strength was more than that of the uncoated ones. The nHAp-coated scaffolds demonstrated the highest compressive strength (2.1 ± 0.17 MPa) compared to the uncoated specimen (0.1 ± 0.05 MPa) [209]. The effect of nHAp particles was evaluated previously. Scaffolds were prepared using compositions of nHAp and PCL. The findings showed that the compressive strength and tensile modulus of the prepared scaffolds containing nHA increased as the weight ratio of nHAp particles increased [210]. In a different investigation, nHAp was applied as a coat on the surface of magnesium-doped wollastonite (CSi-Mg) scaffolds. To examine how surface coating affects the mechanical strength of scaffolds, particularly the relationship between coating thickness and strength, all samples were submerged in an SBF solution for a maximum of three weeks [211]. Distilled water was used to prepare sodium alginate (SA) solutions with varying concentrations of 1.0 %, 1.5 %, and 2.0 % (w/v). To create a 4 % (w/w) solution of nHAp/SA, powders of nHAp were added to the SA solution, while nHAp/ethanol solutions with densities of 0.10 g/ml, 0.15 g/ml, and 0.20 g/ml were created by adding nHAp powders to ethanol. To prepare the CSi-Mg scaffolds, a technique involving immersion in a nHAp/ethanol solution under a vacuum for 2 min was used. The scaffolds were then stirred in the air for a specified amount of time (5 min, 10 min, or 15 min) and dried for 15 min. Next, the scaffolds were submerged in a nHAp/SA solution under a vacuum until no bubbles were present. Over 3 weeks, there was a decrease in compressive strength of about 20% in CSi-Mg scaffolds, which dropped from approximately 91 MPa to 73 MPa. However, the scaffolds coated with nHAp showed a slower decline in compressive strength and maintained a relatively high range of 81–91 MPa even after being immersed for 3 weeks [211]. The composite scaffolds exhibited a consistent pattern: the compressive strength gradually decreased with time. The presence of the nHAp layer resulted in reduced porosity in the scaffolds, improving their mechanical properties. Additionally, the SA component of the nHAp layer dissolved in solution and formed

hydrogels that could fill small gaps on the scaffold's surface, further enhancing its mechanical strength. Such evidence suggests that the increased mechanical durability of the scaffolds was due to the surface adsorption of both nHAp and SA. In conclusion, the CSi-Mg-nHAp composite scaffolds exhibited favorable mechanical stability in a water-based environment and hold promise for use in treating large segmental bone defects [211].

3.5.2. Nano-bioactive glass-ceramics

It was investigated whether applying the BGs (nBGs) nanoparticles created a proximate composition to the natural bone structure. It is supposed that nBGs considerably impact the mechanical characteristics of scaffolds [212]. Combining nBGs with polymers has created a new family of biocomposite materials for TE applications [184]. Esfahani et al. applied a nanocomposite layer of nBG and polycaprolactone (PCL) to the struts of a biphasic calcium-phosphates (BCP) scaffold to enhance its mechanical and biological characteristics. They evaluated the impact of varying concentrations of nBG (ranging from 1 to 90 wt%) on the mechanical properties of the scaffold with two other scaffolds: one coated with PCL and nano-hydroxyapatite (nHAp), and another coated solely with a PCL layer. Adding nBG ranging from 1 % to 90 % by weight produced scaffolds with compressive strengths ranging from 0.2 MPa to 1.45 MPa, and moduli ranging from 19.3 MPa to 49.4 MPa. This pathway was also found for scaffolds containing PCL and nHAp. The maximum compressive strength enhanced approximately 14 times, with moduli approximately three times higher, in the presence of 30 wt% of nBGs compared to BCP scaffolds [213]. Ji et al. stated that the combination of nBGs with PCL affected the elastic modulus and reached 851 ± 43 MPa (the initial value for elastic modulus was 198 ± 13 MPa). It should be mentioned that the concentration of used nBGs was up to 40 %, and their diameter was between 50 and 90 nm [214]. Also, incorporating some ions can increase the mechanical properties of MBG. Boron (B) is one of these. Eder et al. reported that incorporating B_2O_3 in MBG increased hardness and modulus. It was reported that adding 0.5 mol% caused an increase of about 50 % compared to the MBG without B_2O_3 [215]. Boron (B) is one of these. Eder et al. reported that incorporating B_2O_3 in MBG increased hardness and modulus. It was reported that adding 0.5 mol% caused an increase of about 50 % compared to the MBG without B_2O_3 [215].

A similar effect of adding B was observed in Tezcaner et al.'s investigation. A dentin structure was successfully developed using B-modified nBGs and cellulose acetate/oxidized pullulan/gelatin polymers through thermally induced phase separation and porogen leaching for regenerative endodontics. B (7 %, 14 %, and 21 %) and nBG (10 % and 20 %) were added in different amounts. Various scaffold groups' compressive strength and elastic moduli values were determined at 25 % strain on the stress-strain curve. The findings showed the highest compressive strength for scaffold was reported 0.40 ± 0.03 MPa, which contains 14 % and 10 % of B and nBG in order. When nBGs content was increased to 20 %, there was a decrease in the compressive strength and elastic moduli in different groups [216]. Regarding the previous research, adding BG can promote the mechanical properties of nanocomposites [217,218]. Reducing the filler content and smaller nanoparticles (with a higher specific surface area) could improve the bonding between polymers and fillers, thereby increasing the materials' strength and ability to resist deformation [219,220]. Moreover, the nano-58S-BG was used to enhance the mechanical characteristics of β-TCP scaffolds. The compressive strength improved from 3.7 ± 0.27 MPa to 18.2 ± 0.62 MPa after adding 15 wt% of nano-58S-BG. It was reported that more than this amount caused a decrease in the compressive strength [221]. A previous study reported that using nano-size bioceramics significantly affected the mechanical properties compared to the micro size. The bioceramic scaffolds made from the nano-size powder of b-tricalcium phosphate [β-$Ca_3(PO_4)_2$, β-TCP] have a 10.87 MPa compressive strength. It was about twice as many as the micro-size scaffolds produced. The porosity levels were approximately 65 %, with uniformly distributed macropores of 400–550 micrometers. Additionally, the interconnected pore size was around 100 micrometers [144]. Scaffolds belonging to a new category were developed using nanocomposite powders of wollastonite/tricalcium phosphate (WT). These scaffolds, known as "nano-sintered scaffolds," had a grain size of 200 nm and were manufactured through a two-step chemical precipitation and porogen burnout technique. To compare, another type of WT scaffolds, called "submicron-sintered scaffolds," with a grain size of 2 μm, were also fabricated using submicron composite powders under the same conditions. WT nano-sintered scaffolds' mechanical properties were significantly higher than their submicron-sintered counterparts. The nano-sintered scaffolds, with a 50 ± 1.0 % porosity, exhibited a compressive strength of 16.2 ± 3.0 MPa and an elastic modulus of 350 ± 30 MPa. In contrast, the submicron-sintered scaffolds had a compressive strength of only 8.4 ± 2.0 MPa and an elastic modulus of 180 ± 35 MPa. Increasing the porosity from 50 ± 1.0 % to 65 ± 1.0 % resulted in an almost twofold increase in mechanical properties for the nano-sintered scaffolds [222].

3.5.3. Nano MgO and SiO_2 particles

The nanoparticles of MgO and SiO_2 have an essential role in cells' function, which is needed for several applications in tissue repair [213]. Gao et al. employed these nanoparticles to boost and increase the mechanical properties of scaffolds. The incorporation of MgO and SiO_2 particles in the β-TCP scaffolds was carried out in different concentrations. The scaffolds that included both nanoparticles demonstrated the highest compressive strength than those without nanoparticle embedding. It was observed that the inclusion of nanoparticles had a significant impact on the compressive strength of the scaffold. Specifically, compared to the scaffold made solely from β-TCP with a compressive strength of 3.12 ± 0.36 MPa, the incorporation of SiO_2 resulted in a significantly increased compressive strength of 5.74 ± 0.62 MPa. Adding MgO Further increased the compressive strength to 9.02 ± 0.55 MPa. The scaffold with the highest compressive strength of 10.43 ± 0.28 MPa was obtained when both SiO_2 and MgO were included. It was stated that this increase might be because of increasing the density after doping MgO and reducing the α-TCP formation [223].

3.5.4. Nanodiamonds

Nanodiamonds (NDs) are a novel type of carbon-based nanoparticles with desirable chemical and physical properties. NDs are recognized as a valuable and applicable option for increasing the mechanical characteristics of different scaffolds [224]. NDs' incorporation with diverse cell cultures has been investigated. If dispersed adequately, NDs can promote toughness, strength, and nanocomposite thermal stability [19]. A previous study incorporated octadecylamines functionalized ND with scaffolds made of poly-L-lactic acid (PLLA) and observed that the mechanical properties increased even with only 10 wt% of these particles [224].

Collectively, different materials have various impacts on their mechanical properties. Therefore, appropriate material can be chosen based on expected targeted features. Fig. 3 shows a good data scheme for better understanding this impact that covers different materials, not only ceramics but also metals, foams, elastomers, and polymers.

3.6. Combination of bioceramics and polymers

In addition to the description above, combining bioceramics and polymers can be considered a strategy to improve bioceramics' mechanical properties. In one of the case studies of Du et al., a porous multicomponent scaffold was made of PCL coated with chitosan containing wollastonite-HA. Four samples were prepared with different HA weight percentage (the exact content of HA in samples have not been mentioned in this study). FDM prepared samples, and the coating process used the freeze-drying technique. Findings showed that the natural property of HA caused an increase in materials' hardness. As a result, the

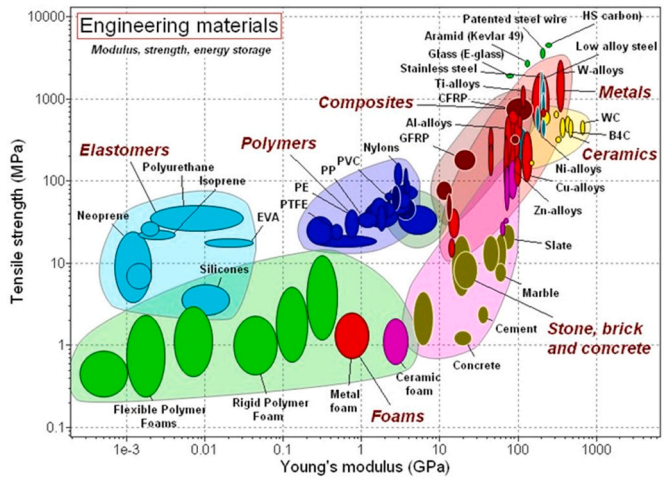

Fig. 3. Comparing Young's modulus (GPa) and the tensile strength (MPa) of different materials [225] Figure reused with permission from Ashby et al., 2008.

0 % HA sample exhibited a hardness of approximately 25, while the 15 % HA sample exhibited a hardness of around 39. An increase from 117 MPa to 149 MPa and 3.5 ± 0.5–4.9 ± 0.6 MPa have been reported for elastic modulus and compressive strength, respectively. The addition of HA stabilized the chitosan solution, composed alongside wollastonite bioceramic [23]. Therefore, it can be concluded that if HA is used with polymers, their mechanical properties can be improved effectively. Another proof of using polymers/bioceramics is fabricated PCL scaffolds reinforced with zinc (Zn)-HA and boron nitride nanofiber designed by Evis et al. recently. One of the aims was to evaluate the effect of adding Zn/HA on the PCL scaffolds, and boron nitride nanofiber was applied to analyze whether it would aid in promoting osteogenesis and increasing cell viability. Four samples with various compositions, including PCL, PCL/Zn/HA, PCL/Zn/HA/ boron nitride nanofiber, and PCL/ boron nitride nanofiber, have been designed. Adding Zn/HA and boron nitride nanofiber affected Young's modulus significantly in both tensile and compression tests compared to other samples. In the tensile test, Young's modulus was 34.66 ± 9.61, 7.65 ± 1.13, 10.73 ± 0.91, and 5.14 ± 1.18 MPa for PCL, PCL/Zn/HA, PCL/Zn/HA/boron nitride nanofiber, and PCL/ boron nitride nanofiber, in order. In the compression test, Young's modulus was 1.38 ± 0.59, 3.42 ± 0.10, 5.54 ± 2.20, and 3.30 ± 0.54 MPa, and the compressive strength was reported as 0.34 ± 0.26, 0.87 ± 0.50, 2.53 ± 3.61, and 1.05 ± 1.02 MPa, in order. PCL/Zn/HA/ boron nitride nanofiber contributed to better mechanical properties [226]. Another study analyzed the effects of the concentration of the multi-doped HA (10 and 20 wt%) and porosity levels (50 % and 60 %) on the mechanical and biological properties of PCL-PEG-PCL/B-Sr-Mg multi-doped HA composite scaffolds. The scaffolds group with 50 % porosity showed higher compressive strength than their counterpart with 60 % porosity. Scaffolds including 2Sr0.5B10%HA (23.31 ± 0.37 MPa), 2Sr0.5B20%HA (24.27 ± 1.14 MPa), and 50 % porosity showed higher compressive strengths among all scaffolds. The compressive strength from the highest to the lowest were for 2Sr0.5BHA, pure HA, 0.5BHA, and 0.5Sr0.75Mg0.5BHA scaffolds, respectively ($p < 0.05$). Notably, scaffolds containing lower porosity and higher HA had better compressive strength ($p < 0.01$) [207].

Zreiqat et al. reported improved mechanical properties of $CaSiO_3$ scaffolds by poly-(D, L-lactic acid) (PDLLA) polymer incorporation. Incorporating the polymer into the $CaSiO_3$ scaffolds resulted in the formation of PDLLA-modified $CaSiO_3$ scaffolds, which showed a substantial enhancement in compressive strength compared to the $CaSiO_3$ scaffolds. In the air, the compressive strength of scaffolds containing PDLLA reached 1450 kPa and decreased slightly to 1100 kPa when tested in phosphate-buffered saline (PBS) solution. In contrast, the compressive strength of the $CaSiO_3$ scaffolds was only 300 kPa, regardless of the testing environment. The degradation of the scaffolds was evaluated by soaking them in PBS solution for different durations (0, 1, 3, 7, and 14 days). As the weight loss increased over time, both the $CaSiO_3$ and $CaSiO_3$- PDLLA scaffolds exhibited a decrease in compressive strength, compressive modulus, and percent strain. However, even throughout the degradation process, the $CaSiO_3$- PDLLA scaffolds consistently demonstrated a significant improvement in compressive strength, compressive modulus, and percent strain compared to the $CaSiO_3$ scaffolds [227]. To enhance the mechanical properties of scaffolds produced through selective laser sintering (SLS), a small quantity (0.5–3 wt%) of PLLA is incorporated into the β-TCP powder. The inclusion of 1 wt% PLLA in the mixture powder results in an 18.18 % increase in fracture toughness and a 4.45 % increase in compressive strength compared to scaffolds made solely from β-TCP powder. This strengthening and toughening effect is attributed to the improved sintering characteristics of β-TCP facilitated by introducing a transient liquid phase during SLS. Additionally, the presence of PLLA inhibits the formation of microcracks caused by volume expansion from the β–α phase transformation of TCP. However, using a PLLA additive exceeding 1 wt% can result in PLLA residue, which diminishes the mechanical properties. Experimental findings demonstrate that PLLA is an effective sintering aid for enhancing the mechanical properties of a TCP scaffold [228].

In conclusion, bioceramics have interesting properties that can be used as scaffolds. But, according to their drawback mentioned in this review, their poor mechanical properties are a barrier. So, using simple bioceramics is not suggested. Section 3 in this work gives some strategies to improve the mechanical properties of bioceramics that are summarized below:

- Incorporating different ions, including zirconia, Cu, B, nitrogen, etc., can promote the bioceramics scaffolds' properties. However, it should be mentioned that while other ions are used, the bioactivity of bioceramics should be controlled, not to disappear.
- Another strategy is using nanoparticles. As mentioned, nBGs, nHAp, nanodiamonds, etc., have a better impact on the mechanical properties. The numbers reported for mechanical properties indicate that using nanoparticles instead of normal-sized particles can overcome the poor mechanical properties. Enhancing the tensile strength of a scaffold relies on achieving a strong affinity between nanoparticles and the scaffold material. A good dispersion of nanoparticles within a scaffold can lead to a larger interfacial area, significantly enhancing fracture energy and other mechanical properties.
- The third solution to improve bioceramics' mechanical properties is the combination of them with polymers, such as PCL and PDLLA. Investigations showed that using a combination of polymers and bioceramics can solve the disadvantages of both of them. Bioceramics can help the bioactivity of composition, and polymers can improve mechanical properties.

3.7. The impact of scaffold modification on mechanical features

Surface modification is one suggested solution to improve scaffolds' mechanical properties [166]. The coating is the most commonly used surface modification. In one case study, coatings with poly-(D, L-lactic acid) (PDLLA)-bioglass or PDLLA were applied on the TiO_2 foam. After coating, the compressive strength increased approximately seven times (~0.3 MPa) compared to the uncoated foam (0.045 MPa) [229]. The main reason for increasing and promoting the mechanical properties of coating has been mentioned: coating plays a crucial role in filling cracks in the struts in foams so they can be thicker [166]. The naturally derived polymer melanin was used to coat glass-ceramics scaffolds and showed better mechanical properties than the uncoated scaffold. The compressive strength reached 1.3 MPa due to the coating (the initial value was 0.5 MPa). The mechanical properties can be improved by filling and

covering the micro-cracks on the surface of the scaffold strut with polymer [230]. Recoating is another method for improving mechanical properties, as it has been shown to fill the gaps, micropores, and remaining folds on the single and first coat. Finally, the slurry was deposited and recoated on the folds and gaps.

Consequently, the struts' thickness increased slightly. Tiainen et al. observed that the TiO_2 foam's strength increased considerably after recoating [156]. Recently, Zhang et al. characterized the effect of PCL impregnation on the properties of CS scaffolds fabricated by 3D printing. PCL has been added in different concentrations of 3 %, 5 %, 7 %, 9 %, and 11 %. Compressive strength was considerably improved by applying PCL coating on CS scaffolds [231]. Compressive strength has been changed from 16.38 MPa to 22.65 MPa by coating the CS scaffold with 3 % PCL, and the mechanical characteristics of scaffolds coated with PCL continued to improve. The compressive strength of scaffolds coated with 11 % PCL has reached 30.63 MPa, more than double that of scaffolds made of CS material without any coatings. Following the compression process, it was observed that scaffolds impregnated with low concentrations of PCL broke apart into multiple parts.

On the other hand, the impregnated scaffolds with a PCL concentration higher than 5 % could keep their original shape and did not fracture even when subjected to greater strains (surpassing 10 %). It has been reported that the porosity of the CS scaffold was 50.3 %. However, after coating the scaffold with PCL, there was a significant reduction in its porosity. Furthermore, an increase in PCL concentration resulted in a decrease in the porosity of the scaffold. For example, scaffolds' porosity with 3 % PCL was 42.9 %, and that of scaffolds with 11 % PCL was 38.4 %. Based on the overcomes obtained, it can be concluded that the PCL coating had a filling effect on the scaffolds' microporous structure. Moreover, with an increase in PCL concentration, a gradual increase was observed in the scaffold filling degree [231]. Salahinejad et al. worked on differences between the impacts of PLGA- and PLA-coated porous bioceramic scaffolds, and their mechanical assessment has been illustrated in Table 4 [232].

Polymer infiltration is another method for promoting mechanical properties. PLA and PCL were applied and infiltrated on the scaffolds, which were fabricated using the robocasting method. Immersing 13–93 scaffolds in polymer melt was found to improve mechanical properties, and the results of PCL and PLA infiltration were also evaluated accurately; however, the effect of this method on the porosity was not reported [243]. Li et al. fabricated the HAp ceramics and incorporated a biopolymer (Polyactive™) into struts using vacuum infiltration. It was reported that mechanical properties improved by combining organic and inorganic phases [244]. Another study also investigated how using PDLLA as a coat for the internal porous HAp's surface affected the mechanical features [245,246]. However, this coat did have bioactivity. So, in one case study, the combination of BGs and PLGA was used for the internal surface of HAp scaffolds. A compressive strength of 4.0—5.8 MPa has been obtained after applying PLGA (initial value: 1.5—1.8 MPa), and BG provided good bioactivity for the fabricated scaffolds [247]. PDLLA and PLGA have been used as a coat for calcium phosphate- and BGs-based scaffolds to boost mechanical features and cover microcracks in the struts previously [227,248,249]. A study investigated the effect of PLA and PCL infiltration of TCP scaffolds on compressive strength. Compressive strength was reported at 130 $\pm$ 20 MPa, 60 $\pm$ 10 MPa, and 20 $\pm$ 2 MPa for PLA/TCP, PCL/TCP, and TCP. PCL infiltration increased compressive strength threefold, and PLA increased sixfold by approximately [160]. Notably, CS ceramics are ideal for reconstructing bone tissue due to their superior bioactivity properties. However, their low mechanical properties present a significant limitation [250]. In the previous sections, a solution was mentioned to improve the mechanical features of these ceramics. However, in this section, another method Wu et al. investigated is the modification of scaffolds based on CS with the application of polymers such as PDLLA. In the previous sections, it has been mentioned that adding B_2O_3 to BGs composition improves the mechanical properties, similar to that reported by Rad et al. Porous scaffolds of pure and B_2O_3 doped BG are infiltrated with cellulose acetate-gelatin (CA-GE) polymer solution. The pure BG scaffolds had an overall porosity of 64.2 %, with compressive strength and Young's modulus of 0.13 MPa and 2.65 MPa, respectively. The B_2O_3-BG (7%) scaffolds' overall porosity, compressive strength, and Young's modulus rose to 67.3 %, 0.20 MPa, and 4.10 MPa. Afer CA-GE infiltration, the porosity of pure BG and B_2O_3-BG (7 %) scaffolds reduced to 59.35 % and 58.9%. However, the compressive strength and Young's modulus of scaffolds dramatically increased after CA-GE polymer infiltration (0.57 ± 0.05 MPa and 11.35 ± 0.98 MPa for BG; 0.82 ± 0.04 MPa and 16.4 ± 0.71 MPa for B_2O_3-BG (7 %)) [251].

It was seen that the network and structure of Ca-Si-based ceramics scaffolds became uniform in comparison with pure CS scaffolds; however, porosity and pore size were maintained. It was reported that the compressive strength enhanced from 330 KPa to 1400 KPa and that CS scaffolds' brittleness decreased [250]. In a different study on HAp scaffolds, two steps were examined to promote and improve mechanical properties. These steps comprised coating scaffolds with polymer again and ceramics [252]. The first coating was hardystonite, while poly (ε-caprolactone fumarate) (PCLF) was chosen for the second coat. A study demonstrated that utilizing a two-step coating process had a remarkable impact on the mechanical characteristics of a material, resulting in a significant increase in its compressive strength from 0.46 $\pm$ 0.1–2.8 MPa and a substantial increase in the modulus of the scaffolds from 108.81 ± 11.12 MPa to 426.1 ± 15.14 MPa [252]. Concerning porosity, after applying the first coat, the porosity changed from

Table 4
Comparison between the PLA and PLGA's effects on bioceramics scaffolds' mechanical properties.

Kind of bioceramics	Effect on mechanical properties
Kind of polymer coating: PLA	
HAp	Young's modulus and compressive strength improved the most, with 79 % and 184 %, respectively[233]
β-TCP	PLA created a thin and complete layer on the TCP microparticle surface. The porous scaffolds were prepared using three-dimensional (3D) printing technology. The compressive strength of the TCP scaffolds reached significantly from 1.70 ± 0.24 MPa to 17.30 ± 3.69 MPa by PLA infiltration[234]
$CaSiO_3$	Compared with CS scaffolds (the average compressive strength was 21.8 MPa), the compressive strength of PLA/CS (38.12 MPa) scaffolds considerably increased[235]
Bioactive glass (45S5)	PLA coatings provided a significant increase in the scaffolds' compressive strength (it has not been mentioned the exact number of compressive strength changes)[236]
Kind of polymer coating: PLGA	
HAp/TCP	HAp/TCP scaffolds (prepared by a polyurethane foam replica method) could withstand maximum compressive stress between 0.05 and 0.07 MPa, whereas scaffolds coated with PLGA had a compressive strength in the range of 0.62–0.79 MPa. The compressive strength of the scaffolds coated with PLGA was considerably higher (by about 10-fold) than those without the PLGA coating[237]
β-TCP	The PLGA infiltration markedly enhanced the compressive strength of β-TCP scaffolds from 2.90 to 4.19 MPa, toughness from 0.17 to 1.44 MPa, and bending strength from 1.46 to 2.41 MPa while retaining an interconnected porous structure with a porosity of 80.65 %[238]
BCP / ZrO_2	The compressive strength of the scaffolds increased from 8.5 0.52 MPa to 11 0.65 MPa when PLGA concentration was increased from 1 to 2 g in the coat's composition[239]
$CaSiO_3$	The compressive strength of PLGA/CS scaffolds was markedly enhanced compared to pure CS scaffolds (it has not been mentioned the exact number of compressive strength changes)[240]
Bredigite ($Ca_7MgSi_4O_{16}$)	The compressive strength of the bredigite scaffold was about 0.15 MPa. The strength of the scaffold reached around 0.75 MPa after PLGA coating[241]
Bioactive glass (58 S)	The compressive strength of 58 S scaffolds was 0.12 $\pm$ 0.03 MPa and reached 0.25 ± 0.05 MPa for PLGA-coated scaffolds[242]

approximately 93 % ± 1 to approximately 89 % ± 1. With the second step, it reached 82 % ± 0.8 [252].

It was investigated that calcium phosphate cement (CPC) scaffolds' compressive strength improved when PEGylated poly (glycerol-sebacate) (PEGS) was applied as a coating. PEGS with different amounts of PEG (0–40 %) were synthesized and then coated on CPC scaffolds. The results were evaluated using the data obtained (Fig. 4). Compressive strength of CPC scaffolds was observed as 0.78 MPa, which increased to 3.82 MPa after the coating. However, applying PEG in the composition had the opposite impact on the compressive strength (Fig. 4: specimens introduced as CPX/Y, X referred to the content of PEG in PEGS, and Y referred to the amount of PEGS in the final scaffold) [253]. Using different polymers as a coat for the BGs- and ceramics-based scaffolds can effectively overcome a low mechanical property. SmartBone®, a bone graft made from bovine sources, has been brought to market by a medical company based in Switzerland. The product is designed to mimic natural bone. It contains a biocompatible polymer coating (poly (L-lactide-co-ε-caprolactone, PLCL)) mixed with bioactive molecules (specifically, RGD-exposing collagen fragments sourced from animal-derived gelatin) [254–257]. Both mechanical (compressive strength > 10 MPa) and biological performance were improved by adding the materials mentioned above [254,257].

In summary, current experimental evidence demonstrates that polymer infiltration is a potential strategy for improving the mechanical properties of bioceramic materials. Infiltration with a ductile polymer such as PCL can effectively address ceramics' inherent brittleness while improving the material's strength. Although polymers' strengthening and toughening effects are more pronounced in fully impregnated structures than in coated scaffolds, a simple polymeric coating still has a significant impact, especially under bending conditions. The presence of the polymer has been demonstrated to provide even greater toughening under flexural stresses [258].

Numerous studies have recently concentrated on enhancing the bioceramics scaffolds' toughness by introducing a biodegradable polymeric phase through full impregnation or coating [109,145,160,259–264]. While these methods undoubtedly improve mechanical properties, they also have drawbacks in terms of the biological performance of the scaffold. Fully impregnating the structure leads to the loss of the osteoconductive surface on bioceramics and can even result in blockage. Even though those characteristics may eventually be recovered since the biodegradable polymer is resorbed after implantation, the scaffolds' osteointegration, healing, and tissue regeneration can still be delayed. A potential solution to the limitation mentioned earlier is creating a porous structure consisting of composite struts with a bioceramic outer shell and a polymeric core at the center. In this approach, the bioceramic's stiffness and the material's toughness should be combined in this unique disposition to create the optimum mechanical properties of both materials without sacrificing the interconnected porosity necessary for bone ingrowth or the bioceramic's osteoconductive surface [120].

4. Conclusion and future perspective

Bone scaffolds are a vital tissue engineering field, and many materials to be applied for this need. Bioceramics have been introduced as the most appropriate materials due to their impressive properties and response to the human body. Many studies present their properties and applications. On the one hand, many attempts are made to fabricate a scaffold for bone repair. On the other hand, all attempts will be in vain if scaffolds cannot withhold the loads they are exposed to before new tissue formation.

Despite their excellent bioactivity, bioceramics suffer from poor mechanical features. Mechanical properties have a critical impact on scaffolding and forming new tissue. Therefore, it is necessary to focus on strategies to improve mechanical properties such as porosity, pore size, methods, sintering temperature, materials, and modifications. Here, we have summarized the recent successes in improving mechanical strength in terms of mechanical stability.

Bioceramics have a bright future in tissue engineering applications. Still, more investigations on all different kinds of bioceramics are required to improve their properties so that their weakness becomes a treatable problem and make them more effective in bone repair.

Although new technologies such as AM have proven valuable for the production of ceramic scaffolds, it is crucial to acknowledge and address the challenges associated with this approach. These challenges include the inherent brittleness of bioceramics, the requirement of high sintering temperatures, and limitations related to printing methods, preoperative planning, and postoperative complications. Effective optimization of scaffold properties can be achieved by controlling various parameters during the manufacturing process. Nevertheless, determining the optimal printing scheme for large scaffolds with complex internal structures has become increasingly challenging, depending on the

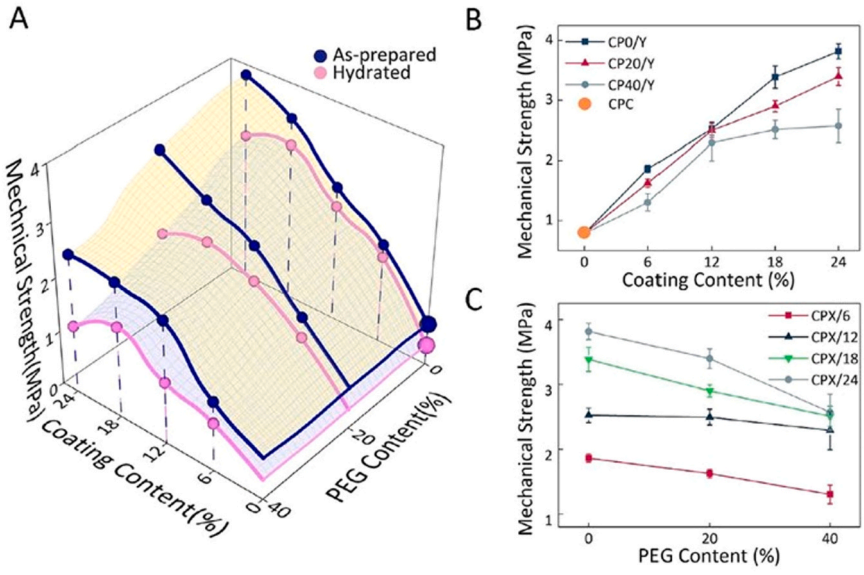

Fig. 4. The effect of coating modification on the mechanical strength of CPC scaffolds. Figure adapted from Ma et al., 2016 [253] and reused in agreement with Elsevier Ltd License number 5271250649269. Copyright © 2016 Acta Materialia Inc. Published by Elsevier Ltd, all rights reserved.

specific scaffold requirements and desired properties. AM technology for bioceramic scaffolds is still in its early stages, necessitating further research efforts to overcome these challenges.

Additionally, the integration of bioceramics with other materials, particularly polymers, holds promise in addressing the inherent weaknesses of bioceramics. However, it is essential to fully consider the natural properties and potential biological risks associated with these polymers when fabricating bioceramic-polymer composite scaffolds on a larger scale. These considerations are pivotal for advancing the field and realizing the potential of bioceramic scaffolds in diverse biomedical applications.

Declaration of Competing Interest

The authors declare that they have no known competing financial interests or personal relationships that could have appeared to influence the work reported in this paper.

Acknowledgments

We acknowledge financial support from the National Natural Science Foundation of China (No. 81971752) and the Baltic Research Program Project No. EEA-RESEARCH-85 “Waste-to-resource: eggshells as a source for next generation biomaterials for bone regeneration (EGGSHELL)” under the EEA Grant of Iceland, Liechtenstein and Norway No. EEZ/BPP/VIAA/2021/1. The authors acknowledge the access to the infrastructure and expertise of the BBCE – Baltic Biomaterials Centre of Excellence (European Union’s Horizon 2020 Research and Innovation Program under grant agreement No. 857287).

References

[1] J.K. Gong JSA, S.H. Cohn, Composition of trabecular and cortical bone, Anat. Rec. 149 (3) (1964) 325–332.
[2] A.L. Boskey SG, C. Gundberg, S.B. Doty, P. Ducy, G. Karsenty, Fourier transform infrared microspectroscopic analysis of bones of osteocalcin-deficient mice provides insight into the function of osteocalcin, Bone 23 (3) (1998) 187–196.
[3] S.J. Jones, A. Boyde, The organization and gross mineralization patterns of the collagen fibres in Sharpey fibre bone, Cell Tissue Res. 148 (1974) 83–96.
[4] X.Y. Zhang, G. Fang, J. Zhou, Additively manufactured scaffolds for bone tissue engineering and the prediction of their mechanical behavior: a review, Materials 10 (1) (2017) 50.
[5] S. Roohani-Esfahani, P. Newman, H. Zreiqat, Design and fabrication of 3D printed scaffolds with a mechanical strength comparable to cortical bone to repair large bone defects, Sci. Rep. 6 (1) (2016) 1–8.
[6] L.C. Gerhardt, A.R. Boccaccini, Bioactive glass and glass–ceramic scaffolds for bone tissue engineering, Materials 3 (7) (2010) 3867–3910.
[7] K. Lin RS, S. Romanazzo, I. Roohani, 3D printing of bioceramic scaffolds – barriers to the clinical translation: from promise to reality, and future perspectives, Materials 12 (17) (2019) 2660.
[8] H.Y.B. Jodatia, Z. Evisa, A review of bioceramic porous scaffolds for hard tissue applications: effects of structural features, Ceram. Int. 46 (10) (2020) 15725–15739.
[9] C.M. Agrawal, R.B. Ray, Biodegradable polymeric scaffolds for musculoskeletal tissue engineering, J. Biomed. Mater. Res. 55 (2) (2001) 141–150.
[10] S. Yang, K.-F. Leong, Z. Du, C.-K. Chua, The design of scaffolds for use in tissue engineering. Part I. Traditional factors, Tissue Eng. 7 (6) (2001) 679–689.
[11] D. Mohamad Yunos, O. Bretcanu, A.R. Boccaccini, Polymer-bioceramic composites for tissue engineering scaffolds, J. Mater. Sci. 43 (2008) 4433–4442.
[12] X. Du, S. Fu, Y. Zhu, 3D printing of ceramic-based scaffolds for bone tissue engineering: an overview, J. Mater. Chem. B 6 (27) (2018) 4397–4412.
[13] Qianli Ma, Zahra Miri, Dagnija Loca, Amirhossein Moghanian, Håvard Jostein Haugen, Significance of mechanical loading in bone fracture healing, bone regeneration, and vascularization, J. Tissue Eng. Regen. M (2023).
[14] C.J. Little, N.K. Bawolin, X. Chen, Mechanical properties of natural cartilage and tissue engineered constructs, Tissue Eng. Part B Rev. 17 (4) (2011) 213–227.
[15] B.P.X. Zhang, C. Zhou, et al., The biomimetic design and 3D printing of customised mechanical properties porous Ti6Al4V scaffold for load-bearing bone reconstruction, Mater. Des. 152 (2018) 30–39.
[16] S. Ma QT, Q. Feng, J. Song, X. Han, F. Guo, Mechanical behaviours and mass transport properties of bone-mimicking scaffolds consisted of gyroid structures manufactured using selective laser melting, J. Mech. Behav. Biomed. Mater. 93 (2019) 158–169.
[17] G.C.J. Turnbull, F. Picard, et al., 3D bioactive composite scaffolds for bone tissue engineering, Bioact. Mater. 3 (3) (2018) 278–314.
[18] A. Song, A.A.R. Karen, L. Christman, Antibacterial and cell-adhesive polypeptide and poly(ethylene glycol) hydrogel as a potential scaffold for wound healing, Acta Biomater. 8 (1) (2012) 41–50.
[19] J. Corona-Gomez, X. Chen, Q. Yang, Effect of nanoparticle incorporation and surface coating on mechanical properties of bone scaffolds: a brief review, J. Funct. Biomater. 7 (3) (2016) 18.
[20] M. Riminucci, P. Bianco, Building bone tissue: matrices and scaffolds in physiology and biotechnology, J. Med. Biol. Res. 36 (8) (2003) 1027–1036.
[21] D.C. Greenspan, Glass and medicine: the Larry Hench story, Int. J. Appl. Glass Sci. 7 (2) (2016) 134–138.
[22] L.L. Hench, Bioceramics, J. Am. Ceram. Soc. 81 (7) (1998) 1705–1728.
[23] X. Du, M. Dehghani, N. Alsaadi, et al., A femoral shape porous scaffold bio-nanocomposite fabricated using 3D printing and freeze-drying technique for orthopedic application, Mater. Chem. Phys. 275 (2022), 125302.
[24] L.L. Hench, Biomaterials: a forecast for the future, J. Biomater. 19 (16) (1998) 1419–1423.
[25] L.L. Hench, R.J. Splinter, W.C. Allen, T.K. Greenlee, Bonding mechanisms at the interface of ceramic prosthetic materials, J. Biomed. Mater. Res. 5 (6) (1972) 117–141.
[26] L.L. Hench, J.M. Polak, Third generation biomaterials, Science 295 (5557) (2002) 1014–1017.
[27] W.R. Lacefield, L.L. Hench, J. Wilson, Introduction to Bioceramics, first ed., World Scientific, 1993.
[28] T. Albrektsson, C. Johansson, Osteoinduction, osteoconduction and osseointegration, Eur. Spine J. 10 (Suppl 2) (2001) S96–S101.
[29] D. Arcos, M. Vallet-Regí, Sol–gel silica-based biomaterials and bone tissue regeneration, Acta Biomater. 6 (8) (2010) 2874–2888.
[30] G. Kaur, G. Pickrell, N. Sriranganathan, V. Kumar, D. Homa, Review and the state of the art: sol-gel or melt quenched bioactive glasses for tissue engineering, J. Biomed. Mater. Res B Appl. Biomater. 104 (6) (2016) 1248–1275.
[31] M. Chabanon, Multiscale Study of a Perfusion Bioreactor for Bone Tissue Engineering [dissertation], Ecole Centrale, Paris, 2015.
[32] G. Altunordu, A. Tezcaner, Z. Evis, D. Keskin, Improvement of bioactivity with dual bioceramic incorporation to nanofibrous PCL scaffolds, Materialia 27 (2023), 101699.
[33] P.V. Giannoudis, H. Dinopoulos, E. Tsiridis, Bone substitutes: an update, Injury 36 (3) (2005) S20–S27.
[34] H.J. Haugen, S.P. Lyngstadaas, F. Rossi, G. Perale, Bone grafts: which is the ideal biomaterial? J. Clin. Periodont. 46 (S21) (2019) 92–102.
[35] A.R. Santos Jr, C.B. Lombello, S.C. Genari, Technologies applied to stimulate bone regeneration, in: J. Davies (Ed.), Tissue Regeneration – From Basic Biology to Clinical Application, InTech, Croatia, 2012, pp. 339–366.
[36] P. Kumar, B.S. Dehiya, A. Sindhu, Bioceramics for hard tissue engineering applications: a review, Int. J. Appl. Eng. Res. 13 (5) (2018) 2744–2752.
[37] A.T. Khalaf, Y. Wei, J. Wan, et al., Bone tissue engineering through 3D bioprinting of bioceramic scaffolds: a review and update, Life 12 (6) (2022) 903.
[38] A.K.S. Kumar, F. Baino, S.S. Han, Additive manufacturing methods for producing hydroxyapatite and hydroxyapatite-based composite scaffolds: a review, Front. Mater. 6 (2019) 313.
[39] S.V. Dorozhkin, Calcium orthophosphate (CaPO4) scaffolds for bone tissue engineering applications, J. Biotechnol. Biomed. Sci. 1 (3) (2018) 25–93.
[40] R.Z. LeGeros, Calcium phosphate-based osteoinductive materials, Chem. Rev. 108 (11) (2008) 4742–4753.
[41] H.F.C. Ma, J. Chang, C. Wu, 3D-printed bioceramic scaffolds: from bone tissue engineering to tumor therapy, Acta Biomater. 79 (2018) 37–59.
[42] L.B.G. Ferrage, P. Lenormand, D. Grossin, B. Ben-Nissan, A review of the additive manufacturing (3DP) of bioceramics: alumina, zirconia (PSZ) and hydroxyapatite, J. Aust. Ceram. Soc. 53 (2017) 11–20.
[43] E. Kolos, A.J. Ruys, Biomimetic coating on porous alumina for tissue engineering: characterisation by cell culture and confocal microscopy, J. Mater. 8 (6) (2015) 3584–3606.
[44] S.M. Kurtz, S. Kocagöz, C. Arnholt, R. Huet, M. Ueno, W.L. Walter, Advances in zirconia toughened alumina biomaterials for total joint replacement, J. Mech. Behav. Biomed. Mater. 31 (2014) 107–116.
[45] R. Galante, C.G. Figueiredo-Pina, A.P. Serro, Additive manufacturing of ceramics for dental applications: a review, Dent. Mater. 35 (6) (2019) 825–846.
[46] M. Bohner, Calcium orthophosphates in medicine: From ceramics to calcium phosphate cements, Injury 31 (2000) D37–D47.
[47] S.V. Dorozhkin, Calcium orthophosphates, J. Mater. Sci. 42 (4) (2007) 1061–1095.
[48] S.V. Dorozhkin, Calcium orthophosphates in nature, biology and medicine, Materials 2 (2) (2009) 399–498.
[49] R.Z. LeGeros, J.P. LeGeros, Calcium phosphate bioceramics: past, present and future, Key Eng. Mater. 240 (2003) 3–10.
[50] S. Pina, R. Rebelo, V.M. Correlo, J.M. Oliveira, R.L. Reis, Bioceramics for osteochondral tissue engineering and regeneration, in: J.Miguel Oliveira Oliveira, P. Sandra, L.R. Rui, R. Julio San (Eds.), Osteochondral Tissue Engineering. Advances in Experimental Medicine and Biology, Springer, Cham, 2018.
[51] N. Eliaz, MNCpbaroth, structure, properties, coating technologies and biomedical applications, Materials 10 (4) (2017) 334.
[52] G.L.O. Daculsi, O. Malard, P. Weiss, Current state of the art of biphasic calcium phosphate bioceramics, J. Mater. Sci. Mater. Med. 14 (3) (2003) 195–200.
[53] F.C.W.F. Ronay, K. Becker, D.B. Wiedemeier, T. Attin, A. Lussi, Pure hydroxyapatite as a substitute for enamel in erosion experiments, J. Dent. 84 (2019) 89–94.

[54] M.G.L. Bohner, N. Doebelin, Calcium phosphate bone graft substitutes: failures and hopes, J. Eur. Ceram. Soc. 32 (11) (2012) 2663–2671.
[55] J.D.M. Lu, J. Dejou, G. Koubi, P. Hardouin, J. Lemaitre, J.P. Proust, The biodegradation mechanism of calcium phosphate biomaterials in bone, J. Biomed. Mater. Res. 63 (4) (2002) 408–412.
[56] S.G.N.F. Kannan, J. Neubauer, J.M. Ferreira, Ionic substitutions in biphasic hydroxyapatite and β-tricalcium phosphate mixtures: structural analysis by Rietveld refinement, J. Am. Ceram. Soc. 91 (1) (2008) 1–2.
[57] S.L.A. Kannan, J.M.F. Ferreira, Synthesis and mechanical performance of biological-like hydroxyapatites, Chem. Mater. 18 (2006) 2181–2186.
[58] S.C. Wu, H.C. Hsu, S.K. Hsu, W.H. Wang, W.-F. Ho, Preparation and characterisation of four different compositions of calcium phosphate scaffolds for bone tissue engineering, Mater. Charact. 62 (5) (2011) 526–534.
[59] H.L.X. Zhang, J. Wen, C. Zhao, Preparation and characterisation of HA/TCP biphasic porous ceramic scaffolds with pore-oriented structure, Ceram. Int 43 (15) (2017) 11780–11785.
[60] L.L. Hench, The future of bioactive ceramics, J. Mater. Sci. Mater. Med. 26 (2015) 1–4.
[61] Dorozhkin S.V. Calcium orthophosphates in nature bamM-.
[62] Q. Ma, K. Rubenis, Ó.E. Sigurjónsson, et al., Eggshell-derived amorphous calcium phosphate: synthesis, characterization and bio-functions as bone graft materials in novel 3D osteoblastic spheroids model, Smart Mater. Med. 4 (2023) 522–537.
[63] L. Chen, P. Qiao, H. Liu, L. Shao, Amorphous calcium phosphate NPs mediate the macrophage response and modulate BMSC osteogenesis, Inflammation 44 (1) (2021) 278–296.
[64] X. Liu, M.N. Rahaman, Q. Fu, Oriented bioactive glass (13-93) scaffolds with controllable pore size by unidirectional freezing of camphene-based suspensions: microstructure and mechanical response, Acta Biomater. 7 (1) (2011) 406–416.
[65] W. B, A new calcium phosphate setting cement, J. Dent. Res. 62 (1983) 672.
[66] M.N. Rahaman, D.E. Day, B.S. Bal, et al., Bioactive glass in tissue engineering, Acta Biomater. 7 (6) (2011) 2355–2373.
[67] J.R. Jones, review of bioactive glass: from Hench to hybrids, Acta Biomater. 9 (1) (2013) 4457–4486.
[68] K. Lobel, L. Hench, In-vitro protein interactions with a bioactive gel-glass, J. Solgel Sci. Technol. 7 (1996) 69–76.
[69] A.A. Gorustovich, J.A. Roether, A.R. Boccaccini, Effect of bioactive glasses on angiogenesis: a review of in vitro and in vivo evidences, Tissue Eng. Part B Rev. 16 (2) (2010) 199–207.
[70] I.D. Xynos, A.J. Edgar, L.D. Buttery, L.L. Hench, J.M. Polak, Ionic products of bioactive glass dissolution increase proliferation of human osteoblasts and induce insulin-like growth factor II mRNA expression and protein synthesis, Biochem. Biophys. Res. Commun. 276 (2) (2000) 461–465.
[71] S.J. Stachelek, I. Alferiev, M. Ueda, E.C. Eckels, K.T. Gleason, R.J. Levy, Prevention of polyurethane oxidative degradation with phenolic antioxidants covalently attached to the hard segments: structure–function relationships, J. Biomed. Mater. Res. A 94 (2010) 751–759.
[72] S.M. Rabiee, N. Nazparvar, M. Azizian, D. Vashaee, L. Tayebi, Effect of ion substitution on properties of bioactive glasses: a review, Ceram. Int. 41 (6) (2015) 7241–7251.
[73] S.K. Nandi, A. Mahato, B. Kundu, P. Mukherjee, Doped bioactive glass materials in bone regeneration, in: A.R. Zorzi, J.B. de Miranda (Eds.), Advanced Techniques in Bone Regeneration, InTechOpen, Croatia, 2016.
[74] A.K.R. Yazdanpanah, F. Moztarzadeh, M. Mozafari, R. Ravarian, L. Tayebi, Enhancement of fracture toughness in bioactive glass-based nanocomposites with nanocrystalline forsterite as advanced biomaterials for bone tissue engineering applications, Ceram. Int. 38 (6) (2012) 5007–5014.
[75] P.W.P. Feng, P. Li, C. Gao, C. Shuai, S. Peng, Calcium silicate ceramic scaffolds toughened with hydroxyapatite whiskers for bone tissue engineering, Mater. Charact. 97 (2014) 47–56.
[76] W. Xue, A. Bandyopadhyay, S. Bose, Mesoporous calcium silicate for controlled release of bovine serum albumin protein, Acta Biomater. 5 (5) (2009) 1686–1696.
[77] Q. Fu, M.N. Rahaman, H. Fu, X. Liu, Silicate, borosilicate, and borate bioactive glass scaffolds with controllable degradation rate for bone tissue engineering applications. I. Preparation and in vitro degradation, J. Biomed. Mater. Res. A 95 (1) (2010) 164–171.
[78] J.C. Knowles, Phosphate based glasses for biomedical applications, J. Mater. Chem. 13 (10) (2003) 2395–2401.
[79] Z.C.X. Xie, C. Zhao, W. Huang, J. Wang, C. Zhang, Gentamicin-loaded borate bioactive glass eradicates osteomyelitis due to Escherichia coli in a rabbit model, Antimicrobial Agents and Chemotherapy 57 (2013) 3293–3298.
[80] R.F.R.M. Brown, A.B. Dwilewicz, W. Huang, D.E. Day, Y. Li, B.S. Bal, Effect of borate glass composition on its conversion to hydroxyapatite and on the proliferation of MC3T3-E1 cells, J. Biomed. Mater. Res. A. 88A (2009) 392–400.
[81] A.M.A. Marikani, M. Premanathan, L. Amalraj, Synthesis and characterization of calcium phosphate based bioactive quaternary P2O5–CaO–Na2O–K2O glasses, J. Non-Cryst. Solids 354 (2008) 3929–3934.
[82] D.M.N.R. Pickup, J.C. Knowles, Sol–gel phosphate-based glass for drug delivery applications, J. Biomater. Appl. 26 (2012) 613–622.
[83] S.F.P. Biamino, M. Pavese, C. Badini, Alumina–zirconia–yttria nanocomposites prepared by solution combustion synthesis, Ceram. Int. 32 (2006) 509–513.
[84] H. Zhao, L. Li, S. Ding, C. Liu, J. Ai, Effect of porous structure and pore size on mechanical strength of 3D-printed comby scaffolds, Mater. Lett. 223 (2018) 21–24.
[85] M. Sayed, E.M. Mahmoud, F. Bondioli, S.M. Naga, Developing porous diopside/hydroxyapatite bio-composite scaffolds via a combination of freeze-drying and coating process, Ceram. Int. 45 (7) (2019) 9025–9031.
[86] P. Deb, E. Barua, A.B. Deoghare, S.D. Lala, Development of bone scaffold using Puntius conchonius fish scale derived hydroxyapatite: physico-mechanical and bioactivity evaluations, Ceram. Int. 45 (8) (2019) 10004–10012.
[87] A.N. Hayati, S.M. Hosseinalipour, H.R. Rezaie, M.A. Shokrgozar, Characterisation of poly(3-hydroxybutyrate)/nano-hydroxyapatite composite scaffolds fabricated without the use of organic solvents for bone tissue engineering applications, Mater. Sci. Eng. C 32 (3) (2012) 416–422.
[88] S.Z.A. Farhangdoust, M. Yasaei, M. Khorami, The effect of processing parameters and solid concentration on the mechanical and microstructural properties of freeze-casted macroporous hydroxyapatite scaffolds, Mater. Sci. Eng. C 33 (2013) 453–460.
[89] Y. Andriani, I.C. Morrow, E. Taran, et al., In vitro biostability of poly (dimethyl siloxane/hexamethylene oxide)-based polyurethane/layered silicate nanocomposites, Acta Biomater. 9 (2013) 8308–8317.
[90] K.E. Styan, D.J. Martin, A. Simmons, L.A. Poole-Warren, In vivo biostability of polyurethane–organosilicate nanocomposites, Acta Biomater. 8 (2012) 2243–2253.
[91] R. Liu, L. Ma, H. Liu, B. Xu, C. Feng, R. He, Effects of pore size on the mechanical and biological properties of stereolithographic 3D printed HAp bioceramic scaffold, Ceram. Int. 47 (20) (2021) 28924–28931.
[92] L.G. Raisz, G.A. Rodan, J.P. Bilezikian, Principles of Bone Biology, second ed., Academic Press,, San Diego, 2002.
[93] Y.H. An, R.A. Draughn (Eds.), Mechanical Testing of Bone and the Bone-Implant Interface, first ed., CRC press, Boca Raton, 1999.
[94] J. Biggemann, M. Pezoldt, M. Stumpf, P. Greil, T. Fey, Modular ceramic scaffolds for individual implants, Acta Biomater. 80 (2018) 390–400.
[95] B. Mondal, S. Mondal, A. Mondal, N. Mandal, Fish scale derived hydroxyapatite scaffold for bone tissue engineering, Mater. Charact. 121 (2016) 112–124.
[96] S. Mondal, G. Hoang, P. Manivasagan, et al., Nano-hydroxyapatite bioactive glass composite scaffold with enhanced mechanical and biological performance for tissue engineering application, Ceram. Int. 44 (13) (2018) 15735–15746.
[97] V. Karageorgiou, D. Kaplan, Porosity of 3D biomaterial scaffolds and osteogenesis, Biomaterials 26 (27) (2005) 5474–5491.
[98] Q. Fu, E. Saiz, M.N. Rahaman, A.P. Tomsia, Toward strong and tough glass and ceramic scaffolds for bone repair, Adv. Funct. Mater. 23 (44) (2013) 5461–5476.
[99] Q. Fu, M.N. Rahaman, B.S. Bal, R.F. Brown, D.E. Day, Mechanical and in vitro performance of 13-93 bioactive glass scaffolds prepared by a polymer foam replication technique, Acta Biomater. 4 (6) (2008) 1854–1864.
[100] Q.Z. Chen, A.R. Boccaccini, D. Poly, L-lactic acid) coated 45S5 Bioglass®-based scaffolds: processing and characterization, J. Biomed. Mater. Res. A 77 (3) (2006) 445–457.
[101] F. Baino, M. Ferraris, O. Bretcanu, E. Verné, C. Vitale-Brovarone, Optimisation of composition, structure and mechanical strength of bioactive 3-D glass-ceramic scaffolds for bone substitution, J. Biomater. Appl. 27 (7) (2013) 872–890.
[102] A. Hoppe, B. Jokic, D. Janackovic, et al., Cobalt-releasing 1393 bioactive glass-derived scaffolds for bone tissue engineering applications, ACS Appl. Mater. Interfaces 6 (4) (2014) 2865–2877.
[103] C. Wu, Y. Zhang, Y. Zhu, T. Friis, Y. Xiao, Structure-property relationships of silkmodified mesoporous bioglass scaffolds, Biomaterials 31 (13) (2010) 3429–3438.
[104] P. Sepulveda, Gelcasting foams for porous ceramics, Am. Ceram. Soc. Bull. 76 (10) (1997) 61–65.
[105] B. Konig Junior, P. Sepulveba, A. Bressiani, J. Bressiani, L. Meseger, In vivo evaluation of hydroxyapatite foams, J. Biomed. Mater. Res. 62 (4) (2002) 587–592.
[106] J.R. Jones, A.R. Boccaccini, Biomedical applications: tissue engineering, in: P. Colombo, M. Scheffler (Eds.), Cellular Ceramics, Structure, Manufacturing, Properties and Applications, Wiley-VCH, Germany, 2005, pp. 547–570.
[107] H.R. Ramay, M. Zhang, Preparation of porous hydroxyapatite scaffolds by combination of the gel-casting and polymer sponge methods, Biomaterials 24 (19) (2003) 3293–3302.
[108] Z.Y. Wu, R.G. Hill, S. Yue, D. Nightingale, P.D. Lee, J.R. Jones, Melt-derived bioactive glass scaffolds produced by a gel-cast foaming technique, Acta Biomater. 7 (4) (2011) 1807–1816.
[109] F. Causa, N. Gargiulo, E. Battista, P.A. Netti, Chapter 13 – Titanium biomedical foams for osseointegration, in: P.A. Netti (Ed.), Biomedical Foams for Tissue Engineering Applications, Woodhead Publishing, Cambridge, 2014, pp. 391–411.
[110] A. Nommeots-Nomm, S. Labbaf, A. Devlin, et al., Highly degradable porous melt-derived bioactive glass foam scaffolds for bone regeneration, Acta Biomater. 57 (2017) 449–461.
[111] T.B.R. Johnson, A. Patel, K. Mequanint, Fabrication of highly porous tissue-engineering scaffolds using selective spherical porogens, Bio-Med. Mater. Eng. 20 (2010) 107–118.
[112] T.A.M. Fukasawa, T. Ohji, S. Kanzaki, Synthesis of porous ceramics with complex pore structure by freeze-dry processing, J. Am. Ceram. 84 (1) (2001) 230–232.
[113] T.D.Z. Fukasawa, M. Ando, T. Ohji, S. Kanzaki, Synthesis of porous silicon nitride with unidirectionally aligned channels using freeze-drying process, J. Am. Ceram. 85 (9) (2002) 2151–2155.
[114] A.F.F. Bigham, E. Rezvani Ghomi, M. Rafienia, R.E. Neisiany, S. Ramakrishna, The journey of multifunctional bone scaffolds fabricated from traditional toward modern techniques, Bio-Des. Manuf 3 (2020) 281–306.
[115] F.I.R. Darus, N. Mamat, M. Jaafar, Techniques for fabrication and construction of three-dimensional bioceramic scaffolds: Effect on pores size, porosity and compressive strength, Ceram. Int. 44 (2018) 18400–18407.

[116] Q. Fu, M.N. Rahaman, F. Dogan, B.S. Bal, Freeze casting of porous hydroxyapatite scaffolds. I. Processing and general microstructure, J. Biomed. Mater. Res B Appl. Biomater. 86 (1) (2008) 125–135.
[117] Osman, N.A.A., Abas, W.A.B.W., Wahab, A.K.A., Ting, H.N., editors. Fabrication of porous ceramic scaffolds via polymeric sponge method using sol-gel derived strontium doped hydroxyapatite powder. In: Proceedings of the 5th Kuala Lumpur International Conference on Biomedical Engineering; 2011 June 20–23; Kuala Lumpur, Malaysia: Springer Berlin Heidelberg;2011.
[118] S. Wu, X. Liu, K.W. Yeung, C. Liu, X. Yang, Biomimetic porous scaffolds for bone tissue engineering, Mater. Sci. Eng. R. Rep. 1 (80) (2014) 1–36.
[119] A. Almirall, G. Larrecq, J. Delgado, S. Martınez, J. Planell, M. Ginebra, Fabrication of low temperature macroporous hydroxyapatite scaffolds by foaming and hydrolysis of an α-TCP paste, Biomaterials 25 (17) (2004) 3671–3680.
[120] C. Paredes, F.J. Martinez-Vazquez, A. Pajares, P. Miranda, Development by robocasting and mechanical characterization of hybrid HA/PCL coaxial scaffolds for biomedical applications, J. Eur. Ceram. 39 (14) (2019) 4375–4383.
[121] A.J. Salinas, M. Vallet-Regí, Bioactive ceramics: from bone grafts to tissue engineering, RSC Adv. 3 (28) (2013) 11116–11131.
[122] I.D. Thompson, L.L. Hench, Mechanical properties of bioactive glasses, glass-ceramics and composites, Proc. Inst. Mech. Eng. H. 212 (2) (1998) 127–136.
[123] S. Esmaeili, H. Akbari Aghdam, M. Motififard, et al., A porous polymeric–hydroxyapatite scaffold used for femur fractures treatment: fabrication, analysis, and simulation, Eur. J. Orthop. Surg. Traumatol. 30 (2020) 123–131.
[124] S. Esmaeili, A. Khandan, S. Saber-Samandari, Mechanical performance of three-dimensional bio-nanocomposite scaffolds designed with digital light processing for biomedical applications, Iran. J. Med. Phys. 15 (2018) 328.
[125] A. Khandan, N. Ozada, Bredigite-Magnetite (Ca7MgSi4O16-Fe3O4) nanoparticles: a study on their magnetic properties, J. Alloy Compd. 726 (2017) 729–736.
[126] L. Dong, A. Makradi, S. Ahzi, Y. Rémond, Three-dimensional transient finite element analysis of the selective laser sintering process, J. Mater. Process Technol. 209 (2008) 700–706.
[127] T.D. Ngo, A. Kashani, G. Imbalzano, K.T. Nguyen, D. Hui, Additive manufacturing (3D printing): a review of materials, methods, applications and challenges, Compos B Eng. 143 (2018) 172–196.
[128] A. Wiberg, J. Persson, J. Ölvander, Design for additive manufacturing – a review of available design methods and software, Rapid Prototyp. J. 25 (6) (2019) 1355–2546.
[129] M. Monshi, S. Esmaeili, A. Kolooshani, B.K. Moghadas, S. Saber-Samandari, A. Khandan, A novel three-dimensional printing of electroconductive scaffolds for bone cancer therapy application, Nanomed. J. 7 (2) (2020).
[130] T. Pepelnjak, J. Stojšić, L. Sevšek, D. Movrin, M. Milutinović, Influence of process parameters on the characteristics of additively manufactured parts made from advanced biopolymers, Polymers 15 (3) (2023) 716.
[131] K. Elhattab, S.B. Bhaduri, P. Sikder, Influence of fused deposition modelling nozzle temperature on the rheology and mechanical properties of 3d printed β-tricalcium phosphate (tcp)/polylactic acid (pla) composite, Polymers 14 (6) (2022) 1222.
[132] Z.U. Arif, M.Y. Khalid, R. Noroozi, A. Sadeghianmaryan, M. Jalalvand, M. Hossain, Recent advances in 3D-printed polylactide and polycaprolactone-based biomaterials for tissue engineering applications, Int. J. Biol. Macromol. 218 (2022) 930–968.
[133] S.H. Riza, S.H. Masood, R.A.R. Rashid, S. Chandra, Selective laser sintering in biomedical manufacturing, in: C. Wen (Ed.), Woodhead Publishing Series in Biomaterials, Elsevier Ltd, Amsterdam, The Netherlands, 2020, pp. 193–233.
[134] A. El Magri, S.E. Bencaid, H.R. Vanaei, S. Vaudreuil, Effects of laser power and hatch orientation on final properties of PA12 parts produced by selective laser sintering, Polymers 14 (17) (2022) 3674.
[135] R.J. Wang, L. Wang, L. Zhao, Z. Liu, Influence of process parameters on part shrinkage in SLS, Int. J. Adv. Manuf. Technol. 33 (2007) 498–504.
[136] L. Dadbakhsh SV, T. Vandeputte, D. Strobbe, P. Van Puyvelde, J.P. Kruth, Effect of powder size and shape on the SLS processability and mechanical properties of a TPU elastomer, Phys. Procedia 83 (2016) 971–980.
[137] E.C.S.M. Santos, K. Osakada, T. Laoui, Rapid manufacturing of metal components by laser forming, Int. J. Mach. Tools Manuf. 46 (2006) 1459–1468.
[138] J.P.L.G. Kruth, F. Klocke, T.H. Childs, Consolidation phenomena in laser and powder-bed based layered manufacturing, CIRP Ann. 56 (2) (2007) 730–759.
[139] K. S, Selective laser sintering: a qualitative and objective approach, JOM 55 (2003) 43–47.
[140] L.D.S. Hao, O. Seaman, M. Felstead, Selective laser melting of a stainless steel and hydroxyapatite composite for load-bearing implant development, J. Mater. Process. Technol. 209 (2009) 5793–5801.
[141] G. Kaur, V. Kumar, F. Baino, J.C. Mauro, G. Pickrell, I. Evans, O. Bretcanu, Mechanical properties of bioactive glasses, ceramics, glass-ceramics and composites: State-of-the-art review and future challenges, Mater. Sci. Eng. C 104 (2019), 109895.
[142] Q. Fu, E. Saiz, A.P. Tomsia, Bioinspired strong and highly porous glass scaffolds, Adv. Funct. Mater. 21 (6) (2011) 1058–1063.
[143] K.A. Hing, Bioceramic bone graft substitutes: influence of porosity and chemistry, Int. J. Appl. Ceram. Technol. 2 (3) (2005) 184–199.
[144] K. Lin, L. Chen, H. Qu, J. Lu, J. Chang, Improvement of mechanical properties of macroporous β-tricalcium phosphate bioceramic scaffolds with uniform and interconnected pore structures, Ceram. Int. 37 (7) (2011) 2397–2403.
[145] A.M. Deliormanlı, M.N. Rahaman, Direct-write assembly of silicate and borate bioactive glass scaffolds for bone repair, J. Eur. Ceram. Soc. 32 (14) (2012) 3637–3646.
[146] X. Liu, M.N. Rahaman, G.E. Hilmas, B.S. Bal, Mechanical properties of bioactive glass (13-93) scaffolds fabricated by robotic deposition for structural bone repair, Acta Biomater. 9 (6) (2013) 7025–7034.
[147] J.C. Wang, H. Dommati, S.J. Hsieh, Review of additive manufacturing methods for high-performance ceramic materials, Int. J. Adv. Manuf. Technol. 103 (2019) 2627–2647.
[148] J.S. Chohan, R. Singh, K.S. Boparai, R. Penna, F. Fraternali, Dimensional accuracy analysis of coupled fused deposition modeling and vapour smoothing operations for biomedical applications, Compos B Eng. 117 (2017) 138–149.
[149] O.A. Mohamed, S.H. Masood, J.L. Bhowmik, Optimization of fused deposition modeling process parameters: a review of current research and future prospects, Adv. Manuf. 3 (1) (2015) 42–53.
[150] O. Abdulhameed, A. Al-Ahmari, W. Ameen, S.H. Mian, Additive manufacturing: challenges, trends, and applications, Adv. Mech. Eng. 11 (2) (2019) 1–27.
[151] M.M.Y. Mirkhalaf, R. Wang, Y. No, H. Zreiqat, Personalized 3D printed bone scaffolds: a review, Acta Biomater. 156 (2023) 110–124.
[152] S. Deville, E. Saiz, A.P. Tomsia, Freeze casting of hydroxyapatite scaffolds for bone tissue engineering, Biomaterials 27 (32) (2006) 5480–5489.
[153] S.K. Swain, D. Sarkar, Preparation of nanohydroxyapatite-gelatin porous scaffold and mechanical properties at cryogenic environment, Mater. Lett. 92 (2013) 252–254.
[154] B. Müller, H. Haugen, S.L. Simonsen, H. Tiainen, Grain boundary corrosion of highly porous ceramic TiO2 foams is reduced by annealing and quenching, J. Eur. Ceram. Soc. 36 (1) (2016) 179–188.
[155] S.A.A. Sadeghpour, M. Hafezi, A. Zamanian, Fabrication of a novel nanostructured calcium zirconium silicate scaffolds prepared by a freeze-casting method for bone tissue engineering, Ceram. Int. 40 (2014) 16107–16114.
[156] H. Tiainen, D. Wiedmer, H.J. Haugen, Processing of highly porous TiO 2 bone scaffolds with improved compressive strength, J. Eur. Ceram. Soc. 33 (1) (2013) 15–24.
[157] J.H. Eom, Y.W. Kim, I.H. Song, H.D. Kim, Microstructure and properties of porous silicon carbide ceramics fabricated by carbothermal reduction and subsequent sintering process, J. Mater. Sci. Eng. A. 464 (1–2) (2007) 129–134.
[158] L. Kaewsichan, D. Riyapan, P. Prommajan, J. Kaewsrichan, Effects of sintering temperatures on micro-morphology, mechanical properties, and bioactivity of bone scaffolds containing calcium silicate, Sci. Asia 37 (2011) 240–246.
[159] F.H. Perera, F.J. Martinez-Vazquez, P. Miranda, A.L. Ortiz, A. Pajares, Clarifying the effect of sintering conditions on the microstructure and mechanical properties of β-tricalcium phosphate, Ceram. Int. 36 (6) (2010) 1929–1935.
[160] D.O. Obada, E.T. Dauda, J.K. Abifarin, D. Dodoo-Arhin, N.D. Bansod, Mechanical properties of natural hydroxyapatite using low cold compaction pressure: effect of sintering temperature, Mater. Chem. Phys. 239 (2020), 122099.
[161] L. de Siqueira, C.G. de Paula, R.F. Gouveia, M. Motisuke, de Sousa, E. Trichês, Evaluation of the sintering temperature on the mechanical behavior of β-tricalcium phosphate/calcium silicate scaffolds obtained by gelcasting method, J. Mech. Behav. Biomed. Mater. 90 (2019) 635–643.
[162] J. Vivanco, J. Slane, R. Nay, A. Simpson, H.L. Ploeg, The effect of sintering temperature on the microstructure and mechanical properties of a bioceramic bone scaffold, J. Mech. Behav. Biomed. Mater. 4 (8) (2011) 2150–2160.
[163] C. Feng, K. Zhang, R. He, et al., Additive manufacturing of hydroxyapatite bioceramic scaffolds: dispersion, digital light processing, sintering, mechanical properties, and biocompatibility, J. Adv. Ceram. 9 (2020) 360–373.
[164] C.H. Chang, C.Y. Lin, F.H. Liu, et al., 3D printing bioceramic porous scaffolds with good mechanical property and cell affinity, PLOS One 10 (11) (2015), e0143713.
[165] J.H.K.W. Lee, T.Y. Yang, S.Y. Yoon, B.K. Kim, H.C. Park, Fabrication of porous ceramic composites with improved compressive strength from coal fly ash, Adv. Appl. Ceram. 110 (2011) 244–250.
[166] S. Novak, J. Druce, Q.Z. Chen, A.R. Boccaccini, TiO2 foams with poly-(d,l-lactic acid) (PDLLA) and PDLLA/Bioglass® coatings for bone tissue engineering scaffolds, J. Mater. Sci. 44 (2009) 1442–1448.
[167] A. Sengottuvelan, P. Balasubramanian, J. Will, A.R. Boccaccini, Bioactivation of titanium dioxide scaffolds by ALP-functionalization, Bioact. Mater. 2 (2) (2017) 108–115.
[168] S. Farhangdoust, A. Zamanian, M. Yasaei, M. Khorami, The effect of processing parameters and solid concentration on the mechanical and microstructural properties of freeze-casted macroporous hydroxyapatite scaffolds, Mater. Sci. Eng. C 33 (1) (2013) 453–460.
[169] J.R. Woodard, A.J. Hilldore, S.K. Lan, et al., The mechanical properties and osteoconductivity of hydroxyapatite bone scaffolds with multi-scale porosity, Biomaterials 28 (1) (2007) 45–54.
[170] I. Sabree, J.E. Gough, B. Derby, Mechanical properties of porous ceramic scaffolds: influence of internal dimensions, Ceram. Int. 41 (7) (2015) 8425–8432.
[171] M.U. Hashmi, S.A. Shah, M.J. Zaidi, S. Alam, Effect of different cao/mgo ratios on the structural and mechanical properties of bioactive glass-ceramics, Ceram. -Silik. 56 (4) (2012) 347–351.
[172] Al-Haidary J.A.-H.M., Qrunfuleh S., Effect of yttria addition on mechanical, physical and biological properties of bioactive MgO–CaO–SiO2–P2O5–CaF2, glass ceramic BM.
[173] S.K. Arepalli, H. Tripathi, S.K. Hira, P.P. Manna, R. Pyare, S.P. Singh, Enhanced bioactivity, biocompatibility and mechanical behavior of strontium substituted bioactive glasses, Mater. Sci. Eng. C 69 (2016) 108–116.
[174] B.A. Ben–Arfa, S. Neto, I.M.M. Salvado, R.C. Pullar, J.M. Ferreira, Robocasting of Cu2+ & La3+ doped sol–gel glass scaffolds with greatly enhanced mechanical

properties: compressive strength up to 14 MPa, Acta Biomater. 87 (2019) 265–272.
[175] A.M.C. Bachar, A. Tricoteaux, S. Hampshire, A. Leriche, C. Follet, Effect of nitrogen and fluorine on mechanical properties and bioactivity in two series of bioactive glasses, J. Mech. Behav. Biomed. Mater. 23 (2013) 133–148.
[176] T.N.K. Kasuga, T. Uno, M. Yoshida, Preparation of zirconia-toughened bioactive glass-ceramic composite by sinter–hot isostatic pressing, J. Am. Ceram. Soc. 75 (1992) 1103–1107.
[177] Y.Z.Y. Zhu, C. Wu, Y. Fang, J. Yang, S. Wang, The effect of zirconium incorporation on the physiochemical and biological properties of mesoporous bioactive glasses scaffolds, Microporous Mesoporous Mater. 143 (2011) 311–319.
[178] A.E.M. Ali, V.K. Vyas, S.K. Hira, P.P. Manna, B.N. Singh, S. Yadav, P. Srivastava, S.P. Singh, R. Pyare, Studies on effect of CuO addition on mechanical properties and in vitro cytocompatibility in 1393 bioactive glass scaffold, Mater. Sci. Eng. C 93 (2018) 341–355.
[179] T. Duminis, S. Shahid, R.G. Hill, Apatite glass-ceramics: a review, Front. Mater. 3 (2017) 59.
[180] M. Montazerian, E. Dutra Zanotto, History and trends of bioactive glass-ceramics, J. Biomed. Mater. Res. A. 104 (5) (2016) 1231–1249.
[181] L. Polo-Corrales, M. Latorre-Esteves, J.E. Ramirez-Vick, Scaffold design for bone regeneration, J. Nanosci. Nanotechnol. 14 (1) (2014) 15–56.
[182] Y.H. An YHA, R.A. Draughn (Eds.), Mechanical Testing of Bone and the Bone–Implant Interface, first ed., CRC Press, Boca Raton, 2000.
[183] K. Schwarz, A bound form of silicon in glycosaminoglycans and polyuronides, Proc. Natl. Acad. Sci. USA 70 (5) (1973) 1608. -1162.
[184] A.R. Boccaccini, M. Erol, W.J. Stark, D. Mohn, Z. Hong, J.F. Mano, Polymer/bioactive glass nanocomposites for biomedical applications: a review, Compos Sci. Technol. 70 (13) (2010) 1764–1776.
[185] C. Wu JC, Silicate bioceramics for bone tissue regeneration, J. Inorg. Mater. 28 (2013) 29–39.
[186] C. Wu, J. Chang, A review of bioactive silicate ceramics, Biomed. Mater. 8 (3) (2013), 032001.
[187] Y. Huang, X. Jin, X. Zhang, et al., In vitro and in vivo evaluation of akermanite bioceramics for bone regeneration, Biomaterials 30 (28) (2009) 5041–5048.
[188] L. Xia, Z. Zhang, L. Chen, et al., Proliferation and osteogenic differentiation of human periodontal ligament cells of akermanite and beta-TCP bioceramics, Eur. Cell Mater. 22 (68) (2011), e82.
[189] X. Liu MNR, Q. Fu, Oriented bioactive glass (13-93) scaffolds with controllable pore size by unidirectional freezing of camphene based suspensions: microstructure and mechanical response, Acta Biomater. 7 (2011) 406–416.
[190] S. Ni, J. Chang, L. Chou, In vitro studies of novel CaO-SiO2-MgO system composite bioceramics, J. Mater. Sci. Mater. Med. 19 (2008) 359–367.
[191] C. Wu, W. Fan, Y. Zhou, et al., 3D-printing of highly uniform CaSiO 3 ceramic scaffolds: preparation, characterization and in vivo osteogenesis, J. Mater. Chem. 22 (24) (2012) 12288–12295.
[192] H. Liu, T.J. Webster, Nanomedicine for implants: a review of studies and necessary experimental tools, Biomaterials 28 (2) (2007) 354–369.
[193] A.S. Coetzee, Regeneration of Bone in the Presence of Calcium Sulfate, Arch Otolaryngol. 106 (7) (1980) 405–409.
[194] S. Sadeghzade, R. Emadi, B. Soleimani, F. Tavangarian, Two-step modification process to improve mechanical properties and bioactivity of hydroxyfluorapatite scaffolds, Ceram. Int. 44 (16) (2018) 19756–19763.
[195] A. Nommeots-Nomm PDL, J.R. Jones, Direct ink writing of highly bioactive glasses, J. Eur. Ceram. Soc. 38 (2018) 837–844.
[196] S. Tajbakhsh, F. Hajiali, A comprehensive study on the fabrication and properties of biocomposites of poly (lactic acid)/ceramics for bone tissue engineering, Mater. Sci. Eng. C 70 (2017) 897–912.
[197] S.K. Padmanabhan, F. Gervaso, M. Carrozzo, F. Scalera, A. Sannino, A. Licciulli, Wollastonite/hydroxyapatite scaffolds with improved mechanical, bioactive and biodegradable properties for bone tissue engineering, Ceram. Int. 39 (1) (2013) 619–627.
[198] Q.S.D. Wei, M. Li, et al., Modification of hydroxyapatite (HA) powder by carboxymethyl chitosan (CMCS) for 3D printing bioceramic bone scaffolds, Ceram. Int. 49 (1) (2023) 538–547.
[199] Q. Li, C. Feng, Q. Cao, et al., Strategies of strengthening mechanical properties in the osteoinductive calcium phosphate bioceramics, Regen. Biomater. (2023), rbad013.
[200] A.D. Dalgic, A.Z. Alshemary, A. Tezcaner, D. Keskin, Z. Evis, Silicate-doped nano-hydroxyapatite/graphene oxide composite reinforced fibrous scaffolds for bone tissue engineering, J. Biomater. Appl. 32 (10) (2018) 1392–1405.
[201] H. Jodati BY, Z. Evis, In vitro and in vivo properties of graphene-incorporated scaffolds for bone defect repair, Ceram. Int. 47 (21) (2021) 29535–29549.
[202] F. Asa'ad, G. Pagni, S.P. Pilipchuk, A.B. Giannì, W.V. Giannobile, G. Rasperini, 3D-printed scaffolds and biomaterials: review of alveolar bone augmentation and periodontal regeneration applications, Int. J. Dent. 2016 (2016) 15.
[203] F. Donnaloja, E. Jacchetti, M. Soncini, M.T. Raimondi, Natural and synthetic polymers for bone scaffolds optimization, Polymers 12 (4) (2020) 905.
[204] N. Mohd, M. Razali, M.J. Ghazali, N.H. Abu Kasim, 3D-printed hydroxyapatite and tricalcium phosphates-based scaffolds for alveolar bone regeneration in animal models: a scoping review, Materials 15 (7) (2022) 2621.
[205] M. Stevanovic, D. Selakovic, M. Vasovic, et al., Comparison of hydroxyapatite/poly (lactide-co-glycolide) and hydroxyapatite/polyethyleneimine composite scaffolds in bone regeneration of swine mandibular critical size defects: in vivo study, Molecules 27 (5) (2022) 1694.
[206] A.Z. Alshemary, A.E. Pazarçeviren, D. Keskin, A. Tezcaner, R. Hussain, Z. Evis, Porous clinoptilolite-nano biphasic calcium phosphate scaffolds loaded with human dental pulp stem cells for load bearing orthopedic applications, Biomed. Mater. 14 (5) (2019), 055010.
[207] B. Yedekçi, A. Tezcaner, B. Yılmaz, T. Demir, Z. Evis, 3D porous PCL-PEG-PCL/strontium, magnesium and boron multi-doped hydroxyapatite composite scaffolds for bone tissue engineering, J. Mech. Behav. Biomed. Mater. 125 (2022), 104941.
[208] A. Abdal-hay, L.D. Tijing, J.K. Lim, Characterization of the surface biocompatibility of an electrospun nylon 6/CaP nanofiber scaffold using osteoblasts, Chem. Eng. J. 215 (2013) 57–64.
[209] S.I. Roohani-Esfahani, S. Nouri-Khorasani, Z. Lu, R. Appleyard, H. Zreiqat, The influence hydroxyapatite nanoparticle shape and size on the properties of biphasic calcium phosphate scaffolds coated with hydroxyapatite–PCL composites, Biomaterials 31 (21) (2010) 5498–5509.
[210] T. Iba, B.E. Sumpio, Morphological response of human endothelial cells subjected to cyclic strain in vitro, Microvasc. Res. 42 (3) (1991) 245–254.
[211] H.J.Z. Shao, P. Xia, et al., 3D-printed magnesium-doped wollastonite/nano-hydroxyapatite bioceramic scaffolds with high strength and anti-tumor property, Mater. Des. 225 (2023), 111464.
[212] M. Erol-Taygun, K. Zheng, A.R. Boccaccini, Nanoscale bioactive glasses in medical applications, Int. J. Appl. Glass Sci. 4 (2) (2013) 136–148.
[213] S.I. Roohani-Esfahani, S. Nouri-Khorasani, Z.F. Lu, R.C. Appleyard, H. Zreiqat, Effects of bioactive glass nanoparticles on the mechanical and biological behavior of composite coated scaffolds, Acta Biomater. 7 (3) (2010) 1307–1318.
[214] L. Ji, W. Wang, D. Jin, S. Zhou, X. Song, In vitro bioactivity and mechanical properties of bioactive glass nanoparticles/polycaprolactone composites, Mater. Sci. Eng. C 46 (2015) 1–9.
[215] L.W.O. Deilmann, B. Cerrutti, et al., Effect of boron incorporation on the bioactivity, structure, and mechanical properties of ordered mesoporous bioactive glasses, J. Mater. Chem. B 8 (7) (2020) 1456–1465.
[216] R.M. Rad, D. Atila, E.E. Akgün, Z. Evis, D. Keskin, A. Tezcaner, Evaluation of human dental pulp stem cells behavior on a novel nanobiocomposite scaffold prepared for regenerative endodontics, Mater. Sci. Eng. C 100 (2019) 928–948.
[217] E. Tavakoli, M. Mehdikhani-Nahrkhalaji, B. Hashemi-Beni, A. Zargar-Kharazi, M. J. Kharaziha, Preparation, characterization and mechanical assessment of poly (lactide-co-glycolide)/hyaluronic acid/fibrin/bioactive glass nano-composite scaffolds for cartilage tissue engineering applications, Procedia Mater. Sci. 11 (2015) 124–130.
[218] M. Otadi, D. Mohebbi-Kalhori, Evaluate of different bioactive glass on mechanical properties of nanocomposites prepared using electrospinning method, Procedia Mater. Sci. 11 (2015) 196–201.
[219] E.M. Lemos, P.S. Patrício, M.M. Pereira, 3D nanocomposite chitosan/bioactive glass scaffolds obtained using two different routes: an evaluation of the porous structure and mechanical properties, Quim. Nova 39 (4) (2016) 462–466.
[220] A. Abdal-hay, K.A. Khalil, A.S. Hamdy, F.F. Al-Jassir, Fabrication of highly porous biodegradable biomimetic nanocomposite as advanced bone tissue scaffold, Arab J. Chem. 10 (2) (2016) 240–252.
[221] S.K. Ramasamy, A.P. Kusumbe, M. Schiller, et al., Blood flow controls bone vascular function and osteogenesis, Nat. Commun. 7 (2016) 1–13.
[222] F.C.J. Zhang, K. Lin, J. Lu, Preparation, mechanical properties and in vitro degradability of wollastonite/tricalcium phosphate macroporous scaffolds from nanocomposite powders, J. Mater. Sci. Mater. Med. 19 (2008) 167–173.
[223] C. Gao, P. Wei, P. Feng, T. Xiao, C. Shuai, S. Peng, Nano SiO2 and MgO improve the properties of porous β-TCP scaffolds via advanced manufacturing technology, Int. J. Mol. Sci. 16 (4) (2015) 6818–6830.
[224] Q. Zhang, V.N. Mochalin, I. Neitzel, et al., Mechanical properties and biomineralization of multifunctional nanodiamond-PLLA composites for bone tissue engineering, Biomaterials 33 (20) (2012) 5067–5075.
[225] M.F. Ashby, The CES EduPack Database of Natural and Man-Made Materials, Cambridge University and Granta Design C,, UK, 2008.
[226] E.A.A.S. Turhan, A. Tezcaner, Z. Evis, Boron nitride nanofiber/Zn-doped hydroxyapatite/polycaprolactone scaffolds for bone tissue engineering applications, Biomater. Adv. 148 (2023), 213382.
[227] C. Wu, Y. Ramaswamy, P. Boughton, H. Zreiqat, Improvement of mechanical and biological properties of porous CaSiO3 scaffolds by poly(d,l-lactic acid) modification, Acta Biomater. 4 (2) (2008) 343–353.
[228] D.Z.J. Liu, C. Shuai, S. Peng, Mechanical properties' improvement of a tricalcium phosphate scaffold with poly-l-lactic acid in selective laser sintering, Biofabrication 5 (2) (2013), 025005.
[229] M.F. Ashby, L.J. Gibson, Cellular Solids: Structure and Properties, second ed., Cambridge University Press,, Cambridge, 1997.
[230] M. Araújo, R. Viveiros, A. Philippart, et al., Bioactivity, mechanical properties and drug delivery ability of bioactive glass-ceramic scaffolds coated with a natural-derived polymer, Mater. Sci. Eng. C 77 (2017) 342–351.
[231] K.W.J. Liu, S. Fang, et al., Effect of polycaprolactone impregnation on the properties of calcium silicate scaffolds fabricated by 3D printing, Mater. Des. 220 (2022), 110856.
[232] A.M. Maadani, E. Salahinejad, Performance comparison of PLA-and PLGA-coated porous bioceramic scaffolds: mechanical, biodegradability, bioactivity, delivery and biocompatibility assessments, J. Control Release 351 (2022) 1–7.
[233] Y. Zusho, S. Kobayashi, T. Osada, Mechanical behavior of hydroxyapatite-poly (lactic acid) hybrid porous scaffold, Adv. Compos Mater. 29 (6) (2020) 587–602.
[234] C. Bergemann, M. Cornelsen, A. Quade, et al., Continuous cellularization of calcium phosphate hybrid scaffolds induced by plasma polymer activation, Mater. Sci. Eng. C 59 (2016) 514–523.

[235] G. Wang, Influence of polydopamine/polylactic acid coating on mechanical properties and cell behavior of 3D-printed calcium silicate scaffolds, Mater. Lett. 275 (2020), 128131.
[236] S. Eqtesadi, A. Motealleh, F.H. Perera, A. Pajares, P. Miranda, Poly-(lactic acid) infiltration of 45S5 Bioglass® robocast scaffolds: chemical interaction and its deleterious effect in mechanical enhancement, Mater. Lett. 163 (2016) 196–200.
[237] X. Miao, D.M. Tan, J. Li, Y. Xiao, R. Crawford, Mechanical and biological properties of hydroxyapatite/tricalcium phosphate scaffolds coated with poly (lactic-co-glycolic acid), Acta Biomater. 4 (3) (2008) 638–645.
[238] Y. Kang, A. Scully, D.A. Young, et al., Enhanced mechanical performance and biological evaluation of a PLGA coated β-TCP composite scaffold for load-bearing applications, Eur. Polym. J. 47 (8) (2011) 1569–1577.
[239] A. Sadiasa, M.S. Kim, B.T. Lee, Poly (lactide-co-glycolide acid)/biphasic calcium phosphate composite coating on a porous scaffold to deliver simvastatin for bone tissue engineering, J. Drug Target 21 (8) (2013) 719–729.
[240] L. Zhao, C. Wu, K. Lin, J. Chang, The effect of poly (lactic-co-glycolic acid)(PLGA) coating on the mechanical, biodegradable, bioactive properties and drug release of porous calcium silicate scaffolds, Biomed. Mater. Eng. 22 (5) (2012) 289–300.
[241] R. Keihan, A.R. Ghorbani, E. Salahinejad, E. Sharifi, L. Tayebi, Biomineralization, strength and cytocompatibility improvement of bredigite scaffolds through doping/coating, Ceram. Int. 46 (13) (2020) 21056–21063.
[242] B. Li, T. Yoshii, A.E. Hafeman, J.S. Nyman, J.C. Wenke, S.A. Guelcher, The effects of rhBMP-2 released from biodegradable polyurethane/microsphere composite scaffolds on new bone formation in rat femora, Biomaterials 30 (2009) 6768–6779.
[243] S. Eqtesadi, A. Motealleh, A. Pajares, F. Guiberteau, P. Miranda, Improving mechanical properties of 13–93 bioactive glass robocast scaffold by poly (lactic acid) and poly (ε-caprolactone) melt infiltration, J. Non Cryst. Solids 432 (2016) 111–119.
[244] S.H. Li, J.R. De Wijn, P. Layrolle, K. De Groot, Toughening of hydroxyapatite through interpenetrating organic/inorganic microstructure, Key Eng. Mater. 240–242 (2003) 147–150.
[245] A.F. Tencer, V. Mooney, K.L. Brown, P.A. Silva, Compressive properties of polymer coated synthetic hydroxyapatite for bone grafting, J. Biomed. Mater. Res. 19 (8) (1985) 957–969.
[246] A.F.W.P. Tencer, J. Swenson, K.L. Brown, Bone ingrowth into ploymer coated porous synthetic coralline hydroxyapatite, J. Orthop. Res. 5 (1987) 275–282.
[247] S. Xu, X. Yang, X. Chen, et al., Effect of borosilicate glass on the mechanical and biodegradation properties of 45S5-derived bioactive glass-ceramics, J. Non Cryst. Solids 405 (2014) 91–99.
[248] Q.Z. Chen, A.R. Boccaccini, Poly(D,L-lactic acid) coated 45S5 Bioglass®-based scaffolds: processing and characterisation, J. Biomed. Mater. Res. 77 (3) (2006) 445–457.
[249] X. Miao, W.K. Lim, X. Huang, Y. Chen, Preparation and characterisation of interpenetrating phased TCP/HA/PLGA composites, Mater. Lett. 59 (29–30) (2005) 4000–4005.
[250] A. Zamanian, S. Farhangdoust, M. Yasaei, M. Khorami, M. Abbasabadi, The effect of sintering temperature on the microstructural and mechanical characteristics of hydroxyapatite macroporous scaffolds prepared via freeze-casting, Key Eng. Mater. 529 (2013) 133–137.
[251] R. Moonesi Rad AZA, Z. Evis, D. Keskin, A. Tezcaner, Cellulose acetate-gelatin coated boron-bioactive glass biocomposite scaffolds for bone tissue engineering, Biomed. Mater. 15 (6) (2020), 065009.
[252] J. Vivanco, H. Lynn Ploeg, Effect of Sintering Temperature on Microstructural Properties of Bioceramic Bone Scaffolds, American Ceramic Society,, 2012, pp. 101–109.
[253] Y. Ma, W. Zhang, Z. Wang, et al., PEGylated poly (glycerol sebacate)-modified calcium phosphate scaffolds with desirable mechanical behavior and enhanced osteogenic capacity, Acta Biomater. 44 (2016) 110–124.
[254] D. D'Alessandro, G. Perale, M. Milazzo, et al., Bovine bone matrix/poly(l-lactic-co-epsilon-caprolactone)/gelatin hybrid scaffold (SmartBone((R))) for maxillary sinus augmentation: a histologic study on bone regeneration, Int. J. Pharm. 523 (2) (2017) 534–544.
[255] E. Facciuto, C.F. Grottoli, M. Mattarocci, et al., Three-dimensional craniofacial bone reconstruction with smartbone on demand, J. Craniofac. Surg. 30 (3) (2019) 739–741.
[256] C.F. Grottoli, A. Cingolani, F. Zambon, R. Ferracini, T. Villa, G. Perale, Simulated performance of a xenohybrid bone graft (SmartBone (R)) in the treatment of acetabular prosthetic reconstruction, J. Func. Biomater. 10 (4) (2019) 16.
[257] A. Cingolani, C.F. Grottoli, R. Esposito, T. Villa, F. Rossi, G. Perale, Improving bovine bone mechanical characteristics for the development of xenohybrid bone grafts, Curr. Pharm. Biotechnol. 19 (12) (2018) 1005–1013.
[258] S. Eqtesadi, A. Motealleh, A. Pajares, F. Guiberteau, P. Miranda, Influence of sintering temperature on the mechanical properties of ϵ-PCL-impregnated 45S5 bioglass-derived scaffolds fabricated by robocasting, J. Eur. Ceram. 35 (14) (2015) 3985–3993.
[259] F.J. Martínez-Vázquez, F.H. Perera, I.V. Meulen, A. Heise, A. Pajares, P. Miranda, Impregnation of β-tricalcium phosphate robocast scaffolds by in situ polymerization, J. Biomed. Mater. Res. A 101 (11) (2013) 3086–3096.
[260] F.J.P.A. Martínez-Vázquez, F. Guiberteau, P. Miranda, Effect of polymer infiltration on the flexural behavior of β-tricalcium phosphate robocast scaffolds, Materials 7 (5) (2014) 4001–4018.
[261] M.G.L. Peroglio, J. Chevalier, L. Chazeau, C. Gauthier, T. Hamaide, Toughening of bio-ceramics scaffolds by polymer coating, J. Eur. Ceram. Soc. 27 (7) (2007) 2679–2685.
[262] M.G.L. Peroglio, C. Gauthier, et al., Mechanical properties and cytocompatibility of poly (ε-caprolactone)-infiltrated biphasic calcium phosphate scaffolds with bimodal pore distribution, Acta Biomater. 6 (11) (2010) 4369–4379.
[263] F.J. Martínez-Vázquez, F.H. Perera, P. Miranda, A. Pajares, F. Guiberteau, Improving the compressive strength of bioceramic robocast scaffolds by polymer infiltration, Acta Biomater. 6 (11) (2010) 4361–4368.
[264] A. Verket, H. Tiainen, H.J. Haugen, S.P. Lyngstadaas, O. Nilsen, J.E. Reseland, Enhanced osteoblast differentiation on scaffolds coated with TiO 2 compared to SiO 2 and CaP coatings, Biointerphases 7 (1–4) (2012) 36.